

NASA Final Report

University of Wisconsin-Madison

Andrew Davis	Paul P.H. Wilson
<code>andrew.davis@wisc.edu</code>	<code>paul.wilson@wisc.edu</code>
Chelsea D'Angelo	Nancy Granda-Duarte
<code>cadangelo@wisc.edu</code>	<code>grandaduarte@wisc.edu</code>

March 16, 2017

Contents

2	Introduction	5
3	CAD Interfaces	6
3.1	The University of Wisconsin Unified Workflow	6
3.2	FluDAG	6
3.3	DagSolid	7
3.4	DagGeant4	7
3.5	HZETran	8
4	Workflows and Tools	9
4.1	ReadOBJ	9
4.2	Generate Hierarchy	9
4.3	Combining Geometries	11
4.4	SRAGCodes	11
5	Benchmarks	16
5.1	ATIC	16
5.1.1	Conclusion	21
5.1.2	AlAuAl	22
5.1.3	Magnetic Field & Spheres	24
6	Analysis	31
6.1	Mars Benchmarks	31
6.1.1	Geometry	31
6.1.2	Workflow	31
6.1.3	Results	32
6.1.4	Conclusion	32
6.2	Topology Calculations	34
6.3	Phantom in Mars Habitat Module	37
A	Materials	40

List of Figures

1	Nested spheres	10
2	Hierarchical tree build from nested spheres geometry.	12
3	Geometry of the input parameters for the Spherical Element source	13
4	Geometry of the ATIC calcualtions native Fluka (left) and FluDAG (right)	16
5	Proton flux profile determine in the native FLUKA geometry (left) and the FluDAG geometry (right)	17
6	Proton flux profiles, FLUKA as lines, FluDAG as points and the ratio of the profiles (FluDAG/Fluka)	17
7	Energy deposition profile determine in the native FLUKA geometry (left) and the FluDAG geometry (right)	18
8	Energy deposition profiles, FLUKA as lines, FluDAG as points and the ratio of the profiles (FluDAG/Fluka)	18
9	Neutron flux profile determine in the native FLUKA geometry (left) and the FluDAG geometry (right)	19
10	Neutron flux profiles, FLUKA as lines, FluDAG as points and the ratio of the profiles (FluDAG/Fluka)	19
11	Photon flux profile determine in the native FLUKA geometry (left) and the FluDAG geometry (right)	20
12	Photon flux profiles, FLUKA as lines, FluDAG as points and the ratio of the profiles (FluDAG/Fluka)	20
13	The geometry of the setup for the AlAuAl benchmark (FLUKA geometry shown)	22
14	22
15	23
16	Geometry of the MagNSphe benchmark showing the incident positron source	24
17	Photon flux determined in the Fluka (left) & FluDAG (right) in the case without magnetic field	25
18	Electron flux determined in the Fluka (left) & FluDAG (right) in the case without magnetic field	26
19	Energy deposition determined in the Fluka (left) & FluDAG (right) in the case without magnetic field	27
20	Photon flux determined in the Fluka (left) & FluDAG (right) in the case with magnetic fields	28
21	Electron flux determined in the Fluka (left) & FluDAG (right) in the case with magnetic fields	29
22	Energy deposition determined in the Fluka (left) & FluDAG (right) in the case with magnetic fields	30
23	Dose Deposition	32
24	Neutron flux for 27 layer and 146 layer model	33
25	Flux at the surface of Mars for proton biased source	33
26	Geometry set up with detectors and atmospheric layers	34
27	Energy deposition in the mountain for protons, neutrons, electrons and positrons	35
28	Energy deposition in the crater for protons, neutrons, electrons and positrons	35
29	Total response at each detector	36
30	Energy deposition in phantom	38

List of Tables

1	Source sampling options for the Spherical Element Source	14
2	Source sampling options for the Spherical source	14
3	Source sampling options for the Spherical source	14
4	Source sampling options for the Spherical source	14

2 Introduction

This report covers the work performed at UW in Wyle Contracts xx & xx. The work can be broken down into the following sections;

- CAD Interface Development
- Workflows & Tools
- Benchmarking Activities
- Analysis

Section 3 discusses the development work that was performed the development of The University of Wisconsin Unified Workflow (3.1) a workflow that facilities the use of DAGMC geometries, material definitions & tally specifications in multiple Monte Carlo (MC) codes. The development of FluDAG is covered in Section 3.2. Updates made to the DagSolid implementation of a Tessellated Solid for Geant4 can be found in Section 3.3, related to DagSolid the DagGeant4 executable can be found in Section 3.4.

Section 4 discusses the workflows & tools that were developed as part of this work. This includes the development of the ReadOBJ method in MOAB for the reading of OBJ files, found in Section 4.1. A tool to generate hierarchical information from OBJ like geometries was developed called GenerateHierarchy and is discussed in Section 4.2. UW made contributions to GCR source development in the SRAGCodes repository and is discussed in Section 4.4.

In order to prove the correctness of FluDAG several benchmarks were performed and are discussed in Section 5.

UW also provided results for a number of different sets of analysis, these can be found in Section 6.

3 CAD Interfaces

3.1 The University of Wisconsin Unified Workflow

The University of Wisconsin Unified Workflow, known as UW² is a mechanism by which monte carlo code agnostic metadata can be attached into DAGMC [1] geometry. A DAGMC geometry file is a MOAB [2] database, which when on disk resides as a HDF5 formatted file. The C++ parts of the Python for Nuclear Engineering (PyNE) toolkit are used as a *Lingua Franca* to aid in the translation of metadata. Specifically, we use the Material, Tally, Particle and Name classes.

Materials

The Material class is the most fundamental class is used in UW², where we create and store materials in their in memory (object) form, and also where the I/O methods are for the writing of the material object. The material object exists as a standard map of integer nuclide ID numbers and their appropriate mass fractions, when required we have functions available to call which will write their MC code specific versions, for example to Fluka or MCNP.

Tallies

`uwuw_prepoc`

The general workflow of using UW² is to make a PyNE material library which contains all the materials which are used in your problem. The `uwuw_prepoc` tool is then used to extract the material objects from the material library and inserts them into the DAGMC geometry file. This DAGMC geometry file can now be run in any of the UW² enabled MC codes, but with the knowledge that the same original material description is used in each code.

Limitations of UW²

It should be noted, that using the UW² workflow inputs the same material description, but the MC code may not be capable of describing the material in its original description, for example whilst Fluka can describe any nuclide arbitrarily by defining its density, atomic and nucleon number it only contains a limited selection for neutron cross sections below 20 MeV, with only the isotopes of hydrogen, helium, lithium, boron, iodine, xenon, caesium, uranium and some of plutonium described in any isoptopic way. This means that physics aside, the “low energy” neutron material definitions are inherently different, but this is order to match the requirements of the physics code and not a limitation of the workflow itself. Similarly to Fluka, Geant4 when suitable neutron transport cross sections are not available it will choose some defaults using the cross sections of nuclides with similar nucleon numbers and atomic numbers.

3.2 FluDAG

The DAGMC implementation using Fluka [3] is known as FluDAG. It uses the FluGG [4] interface that exists in FLuka. The function wrappers have distinct simple C style function arguments and store any C++ state

behind this layer. The FluGG interface was originally written under the assumption that unambiguous results to any of the geometric query functions can be given, such as given a particle location, determine the cell it is bounded by. With DAGMC we need to include some additional state, stored in the RayHistory class which contains information regarding the last triangle that was crossed, this state (if used) should be reset when we change direction, cross boundaries, and when a history ends. There is some complexity regarding the internal program flow of Fluka, Specifically some of the logic of electrons transport “sensing steps” and regarding when particles cross boundaries. Especially electrons crossing boundaries, which can logically cross a boundary but end up in the cell in which it began. The combination of DAGMC state and the need to know when a particle was taking a sensing step means that we needed to access a some of the internal Fluka common blocks which complicates some of the software library design.

3.3 DagSolid

The DAGMC implementation for the Geant4 [5] interface was originally written by the University of Seoul. As part of this contract the *DagSolid* [6] implementation was improved upon, modernised, and a suite of unit tests added. A single instance of a *DagSolid* object performs queries only on a single DAGMC volume, this fits well with the paradigm of Geant4 geometries being hierarchical geometry objects where parent-child relationships indicate which volumes are bounded by others. The *DagSolid* library therefore meets the expectations of the Geant4 geometry interface, it is entirely possible therefore to mix DAGMC geometry and Geant4 geometry seamlessly as the *DagSolid* object will have parents and children well described by Geant4 geometry hierarchy, excellent speedup was observed when used in this mode.

3.4 DagGeant4

Also to facilitate a better user experience, a dedicated *DagGeant4* executable was written which allows the loading and running of the UW² workflow, reading material objects and tallies from the geometry and instantiates the appropriate Geant4 G4Elements, G4Isotopes and G4Materials and implements an appropriate set of G4SensitiveDetector. The *DagGeant4* executable has not been formally benchmarked as part of this work and should be planned as some future work.

Limitations

As described in 3.3 a single *DagSolid* object represents a single DAGMC volume, and allows all the needed geometric query functions that Geant4 expects. However, because of the nature of the production route of DAGMC geometries, i.e. a flat geometry hierarchy where imprinted surface information determines the next volume a ray crosses given a surface, we have no knowledge of any underlying geometry hierarchy. Indeed the typical production route of DAGMC geometry removes all hierarchical information, therefore all *DagSolid* volumes in *DagGeant4* exist as children of the highest level “Mother” volume. This implies a drastic performance hit as *DagGeant4* performs intersections on all volumes at the current level ¹ and the accepted hit is the nearest intersection, thus utterly defeating the full acceleration allowed by the OBB Tree. Instead either

¹Geant4 has a smart voxel builder, which should make this query faster than a linear check of each volumes, but it currently unknown if a *DagSolid* returns enough information for the voxel builder.

the G4Navigator needs to be stateful, keeping track of last surface crossed and therefore making use of the imprint information, or perhaps use *GenerateHierarchy* to allow the use of Geant4 parent-child links.

3.5 HZETran

4 Workflows and Tools

4.1 ReadOBJ

DAGMC ultimately performs transport on a triangulated surface mesh representation of a solid geometry. The mesh is a collection of vertices which connect to make faces, these faces can be organized into surfaces and closed surfaces can represent a volume. ReadOBJ is a tool created to read in a Wavefront OBJ geometry file and populate a MOAB instance with the mesh data in the file. The contents of an OBJ file can vary [?] and this reader was written to support a specific subset of the full file structure.

The line types supported by this reader include object, group, face, and vertex, but there are many other valid obj line types. In the case that a valid, but unsupported line type is read in, it will simply be ignored. If a line is read in and the type is unrecognized, an error will be produced to alert the user and the program will end.

The choice to support these four line types was made because 1) they are common to many OBJ files and 2) specific to this project, all the information needed to convert the phantom voxel data to an hdf5 file can be organized into these types. Objects and groups are both collections of faces. The difference established here is that a group is a generic collection, while objects are thought to be a collection of faces that form a closed surface. OBJ files are organized such that all mesh data that follow an object or group line belong to that object or group. When the reader parses the obj file and an object or group line is found, a new MOAB meshset is created. Meshsets for groups are assigned a name and ID tag and the faces listed below it become members of this meshset. Because an object represents a volume enclosed by a surface, a second meshset is created so there is one for the surface and one for the volume. The volume and surface meshsets are connected through a parent-child relationship. In addition to a name and ID, these meshsets are also given a category and dimension tag. The surface meshset has the faces below the object line as members. Instead of adding the vertices to individual meshsets, they are instead added to a global vertex meshset.

4.2 Generate Hierarchy

For successful radiation transport, all space needs to be explicitly defined by a single material. Geometry files that only contain surface mesh data and no sense of hierarchy amongst these surfaces have inadequate information. More specifically, there is no information about which surfaces are inside, outside, or beside each other. Generate_hierarchy is a class within MOAB [?] that was created to make these files suitable for radiation transport calculations. This tool determines the spatial relationship amongst surfaces and then applies a hierarchical structure based upon those relationships. As an example, Figure 1 depicts a 2D slice of nested surfaces. Consider surface B. It is completely enclosed by surface A, encloses surface D, and is beside surface C. These hierarchical relationships are necessary so that volumetric entities can be determined. For example, it can now be inferred that volume B is the space enclosed by surface B, but outside of surface D.

There are a few fundamental assumptions made about the geometry file read in by this tool. It is assumed that each surface meshset represents a closed surface, that there are no overlapping surfaces, and that there is a volume meshset that exactly corresponds to each surface meshset. It is also assumed that the only hierarchical relationships that exist are the parent-child relationships between volume and surface meshsets and that the surface meshset has forward sense with respect to its corresponding volume meshset. The Generate_hierarchy class has two main public-facing functions build_hierarchy and construct_topology that can be used in sequence to prepare a surface mesh geometry for MC radiation

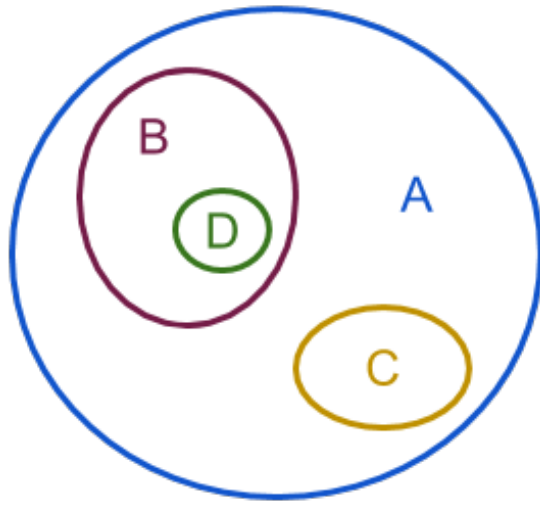


Figure 1: Nested spheres

transport.

Build hierarchy tests every surface in the geometry and decides where it belongs in a hierarchical tree. The hierarchical relationships will actually be made between volume meshsets which at this point, are the meshsets that exactly correspond to the surface meshsets. The tree is formed by testing a point on the surface coming into the tree against the volumes already in the tree. Looking again at Figure 1, lets assume that surface A is the first to be tested. The tree is initially empty so volume A is automatically placed at the top. Assume surface C is tested next. It is found to be inside of volume A, so it becomes a child. Surface D is next and found to also be inside volume A, but neither inside or outside of volume C. Volume D becomes another child

of A. Last, surface B is tested. It is found to be inside of A, outside of B, and beside C. Therefore, volume B becomes a child of volume A, and a parent of volume D. Because a volume can only have one parent, the parent-child linkage between volume A and volume D is broken. The constructed tree is shown in Figure 2 below.

After the hierarchical structure has been established, DAGMC-appropriate volumes are created by `construct_topology`. This is accomplished by setting the surface sense and creating the hierarchical parent-child linkages between the surface meshsets. Each surface has two volumes associated with it, one inside and one outside. The surface has sense forward with respect to the volume it encloses and as mentioned earlier, this is already set. This function sets the reverse sense of the surface to the volume directly above it in the tree. For example, surface B has forward sense with respect to volume B and reverse sense with respect to volume A. Because surface A is the outermost surface, it has forward sense with respect to volume A and no reverse sense. Surfaces that do not have reverse sense set lie in the implicit compliment.

4.3 Combining Geometries

The `combine_geoms` tool [?] was created for cases in which pieces of the full geometry are created separately and then need to be combined together for the final radiation transport calculation. Each piece of the full geometry has its own set of meshsets that are usually assigned a global ID that is an integer between 1 and n, where n is the total number of meshsets in that piece. When several pieces of geometry are combined, the global ID of each meshset needs to be reassigned a unique ID in order to avoid any overlap in ID space. This tool loads each piece of the geometry and then renames the global ID of every MOAB surface and volume meshset.

4.4 SRAGCodes

The SRAGCodes repository is a software library that allows sampling of Galactic Cosmic Ray (GCR) spectra for any Monte Carlo code. The library is written with C++ interfaces and coded using the C++11 standard. The repository contains GCR spectra for Badhwar O'Neill 2014 Model (BOM), Local Interstellar Spectrum, and the 1996 BOM model.

Build SRAGCodes

To build the SRAGCodes repository, first clone the git repository from <https://github.com/kerrylee01/SRAGCodes.git>

```
cd SRAGCodes
mkdir bld
cd bld
cmake .. -DCMAKE_INSTALL_PREFIX=..
make -j
make install
make test
```

The above listing shows the full install procedure including the running of the installation tests. In order to build Fluka with the SRAGCodes linked in run the `build_fluka` script found in the base directory of the SRAGCodes repository.

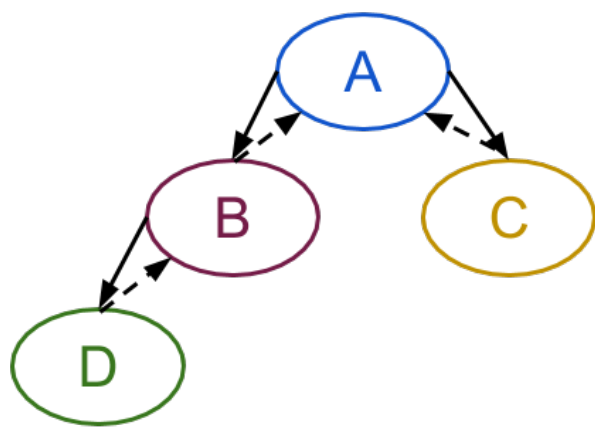


Figure 2: Hierarchical tree build from nested spheres geometry.

Running Fluka with SRAGCodes

First, you must set the GCR_SOURCE_PATH environment variable to tell the Fluka executable where to find the GCR data.

```
export GCR_SOURCE_PATH=/ path / to / SRAGCodes / RadSource / GCRSource /
```

In the Fluka input you wish to run you must add the source description, there are currently two main types of geometric sampling, Spherical Element where you specify a target area and source radius and Sphere where an isotropic inward directed. The geometry of the spherical element source is shown in Figure 3.

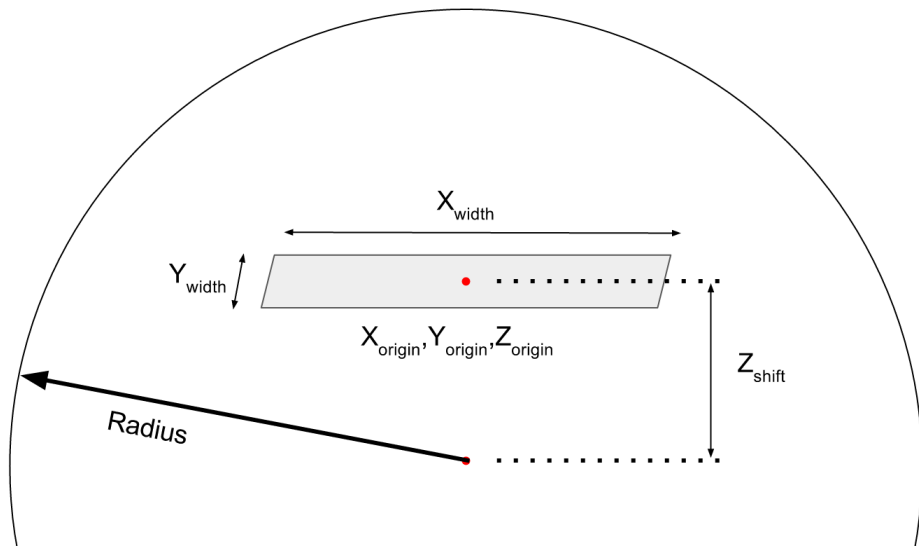


Figure 3: Geometry of the input parameters for the Spherical Element source

Please note that the vertical shift is relative to the origin, so negative values mean the sphere origin is moved below the target plane and positive values are above the source plane. Source particles are sampled by picking a random x,y coordinate in the range of the widths, a ray direction is isotropically sampled in the positive z direction, and this ray is then intersected with the sampling sphere, this intersection point marks the start x,y,z coordinate of the source particle, the direction is similarly defined. The particle weight is then set based on the solid angle of the target area from the intersection point, which effectively defines the probability of any source particle at this point intersecting with the target area. Please note that since particles are traced back from the target rectangle to the source sphere, particles are therefore sampled such that particles are born only above the visible horizon.

Particle ID

Both of the source sampling methods require the entry of the particle id to sample,

Source Type

Both of the source sampling methods require the entry of the source type to sample

Entry	Value
SDUM	SPHELE
WHASOU(1)	X Origin (cm)
WHASOU(2)	Y Origin (cm)
WHASOU(3)	Z Origin (cm)
WHASOU(4)	X Width (cm)
WHASOU(5)	Y Width (cm)
WHASOU(6)	Radius (cm)
WHASOU(7)	Z Shift (cm)
WHASOU(8)	Particle ID to sample
WHASOU(9)	Source Type

Table 1: Source sampling options for the Spherical Element Source

Entry	Value
SDUM	SPHERE
WHASOU(1)	Radius (cm)
WHASOU(8)	Particle ID to sample
WHASOU(9)	Source Type

Table 2: Source sampling options for the Spherical source

Entry	Result
0	sample all particles according to PDF
1	hydrogen isotopes only
2	helium isotopes only
...	...
28	nickel isotopes only

Table 3: Source sampling options for the Spherical source

Entry	Result
0	BOM Jan 2003
1	BOM 2014 from 11/15/2015 to 1/15/2016
2	BOM 2014

Table 4: Source sampling options for the Spherical source

Source Sampling

The main C++ layers of the SRAGCodes library is hideen behind a C safe callable routine that can be linked against C/C++ and Fortran codes. The two functions exposed are `setup()` and `sample()`.

setup

The setup function is necessarily long as we have to pass simple inputs to more complex C++ structures in the SRAGCodes layer.

```
void setup_(double &origin_x, double &origin_y, double &origin_z,
            double &x_width, double &y_width, double &radius,
            double &z_shift, int &ionid, int &spectrum_type, int &error,
            char* src_type, int &string_length)
```

sample

```
void sample_source_(double *randoms, int& num_randoms, double &xxx,
                    double &yyy, double &zzz, double &uuu,
                    double &vvv, double &www, double &energy,
                    double &weight, double &atomic_mass,
                    int &ionID, int &charge, int &nucleon_num)
```

There are two main ways of sampling from the source routine, either pass in a populated vector of uniformly distributed random numbers e.g. double array[6]; or double precision array(6) and set the num_randoms variable to 6, or you can use the internal C++11 random number generator by passing an array and setting num_randoms to 1. The source routine will then return to you an appropriately distributed particle start coordinate xxx,yyy,zzz and noramlised direction vectors uuu,vvv,www. The energy returned in the energy variable is in GeV, the statistical weight weight is a weight between 0 and 1. The ionId variable is Fluka specific and lets fluka know if it is a heavy ion or not, in Fluka heavy ions are defined as particles with greater atomic number than 2. The atomic mass, charge and nucleon number serve to uniquely indentify the particle returned from the sampling routine.

5 Benchmarks

Over the course of the development of FluDAG a number of benchmarks were performed, as a validation of the proof of the functionality of FluDAG the ATIC benchmarking was performed. At the request of CERN the AlAuAl & MagNSphere benchmarks were performed to demonstrate the correctness for electron transport specifically in thin geometries or near boundaries.

5.1 ATIC

The Advanced Thin Ionization Calorimeter (ATIC) detector was a cosmic ray detector flow by high altitude balloon in a number of campaigns from the year 2000 onwards. The geometry existed in a Geant4 geometry and Fluka formats, it was decided by NASA that this geometry, shown in Figure 4, would be used to validate the FluDAG code. The Fluka geometry was used as the canonical geometry format, using Flair the Fluka

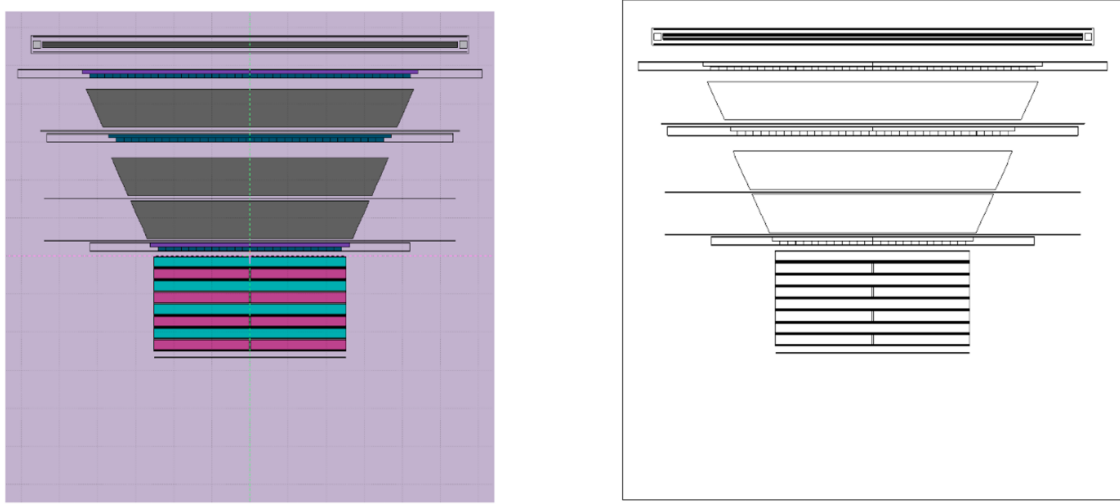


Figure 4: Geometry of the ATIC calcualtions native Fluka (left) and FluDAG (right)

geometry was translated to MCNP format and then subsequently translated to CAD using `mcnp2cad`. This geometry was then assigned appropriate ‘group names’ for FluDAG and then faceted to produce the geometry file. This geometry was then used in all of the FluDAG calculations.

Results

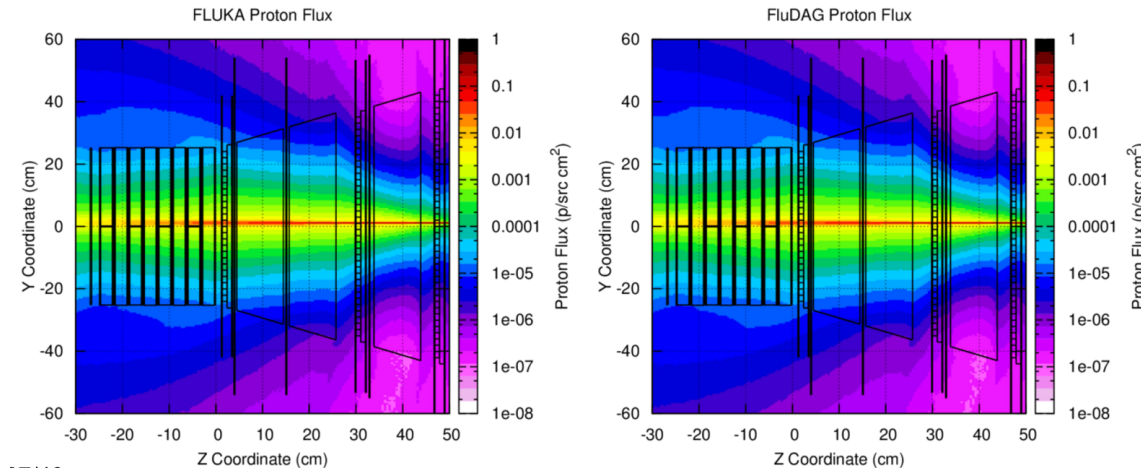


Figure 5: Proton flux profile determine in the native FLUKA geometry (left) and the FluDAG geometry (right)

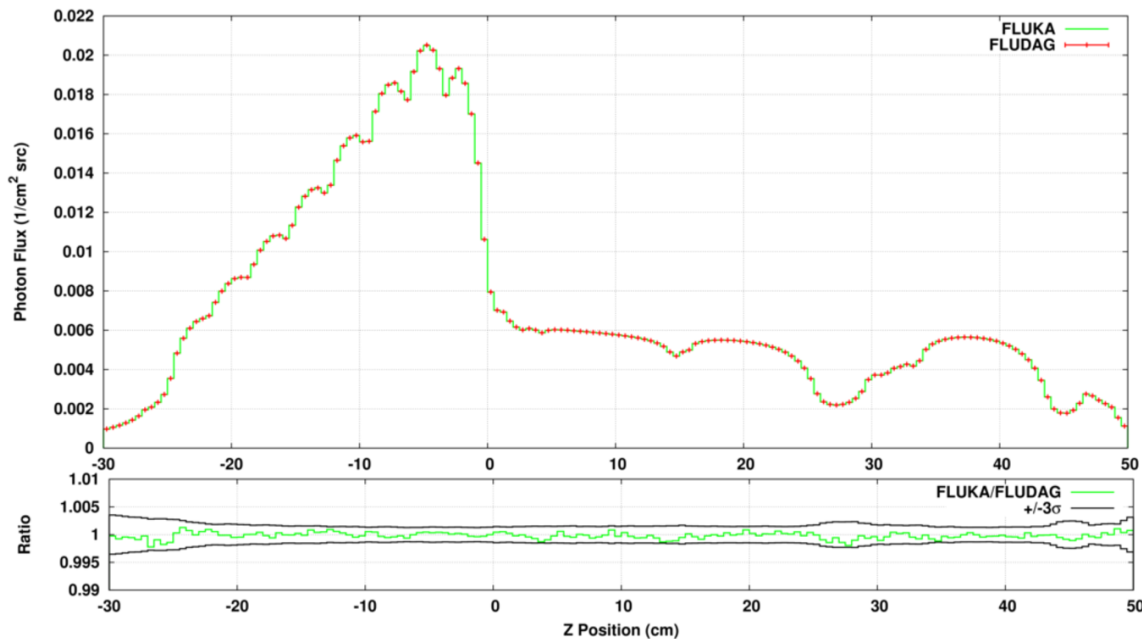


Figure 6: Proton flux profiles, FLUKA as lines, FluDAG as points and the ratio of the profiles (FluDAG/Fluka)

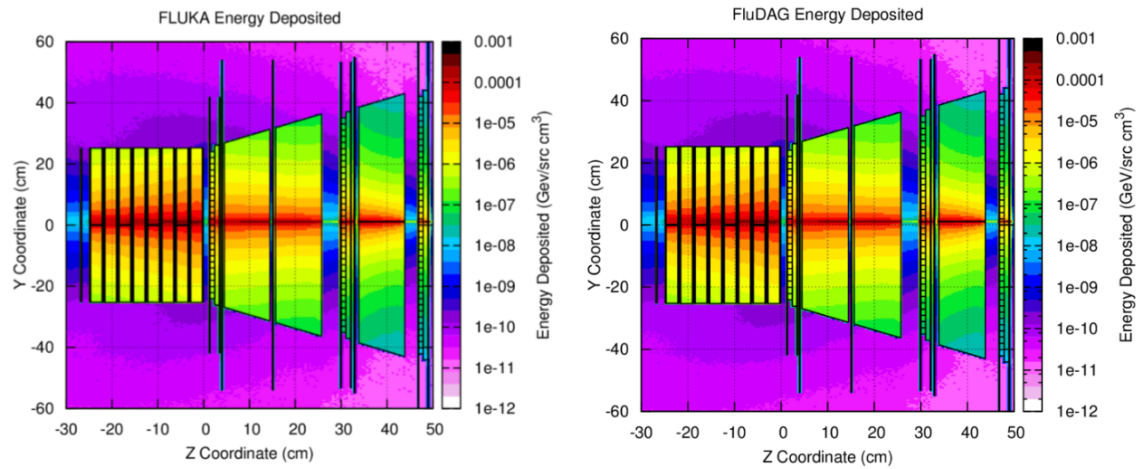


Figure 7: Energy deposition profile determine in the native FLUKA geometry (left) and the FluDAG geometry (right)

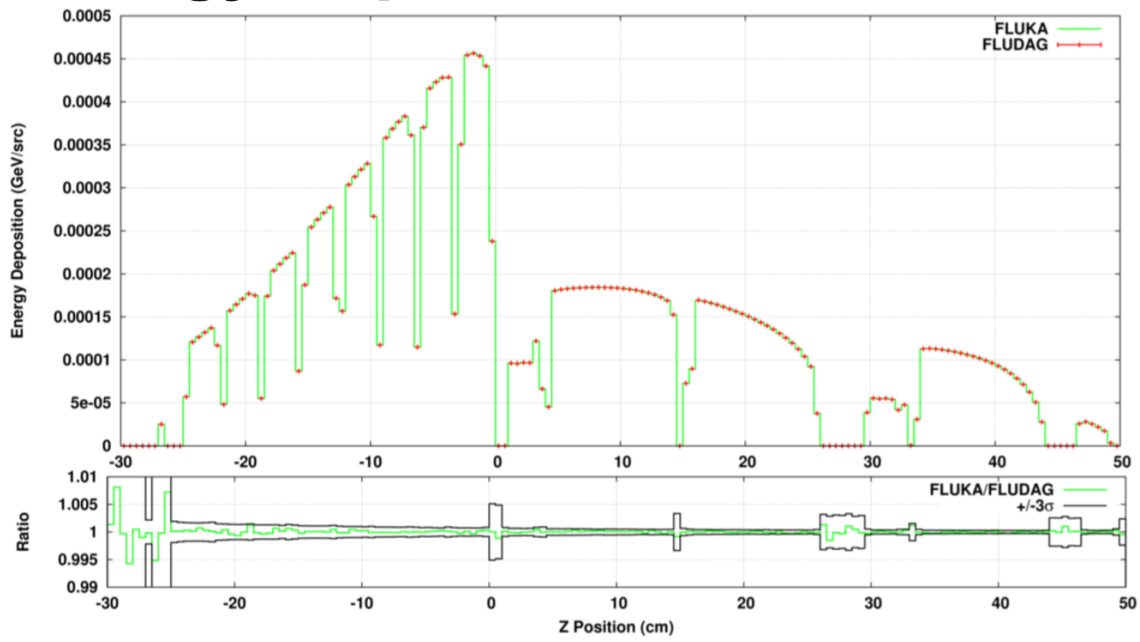


Figure 8: Energy deposition profiles, FLUKA as lines, FluDAG as points and the ratio of the profiles (FluDAG/Fluka)

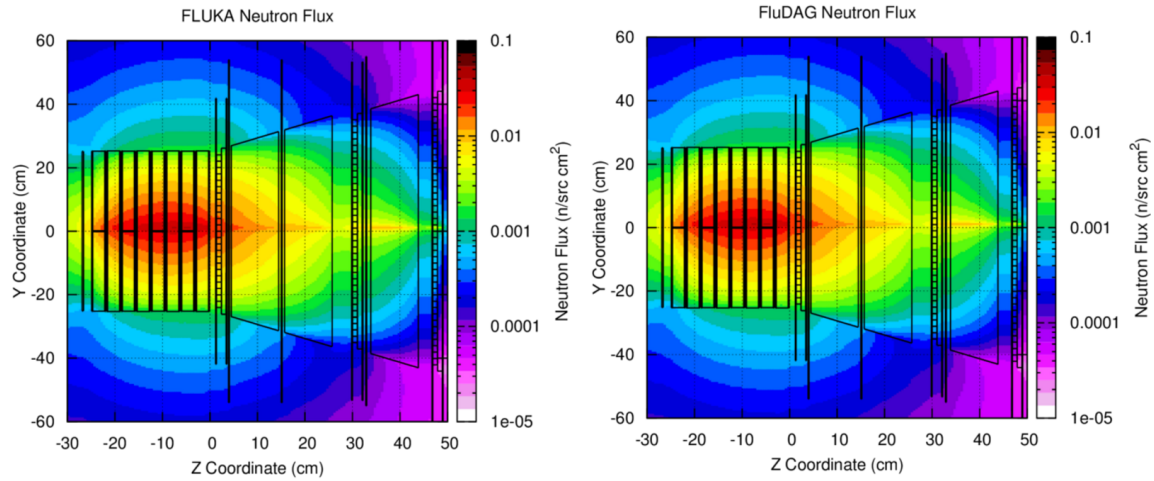


Figure 9: Neutron flux profile determine in the native FLUKA geometry (left) and the FluDAG geometry (right)

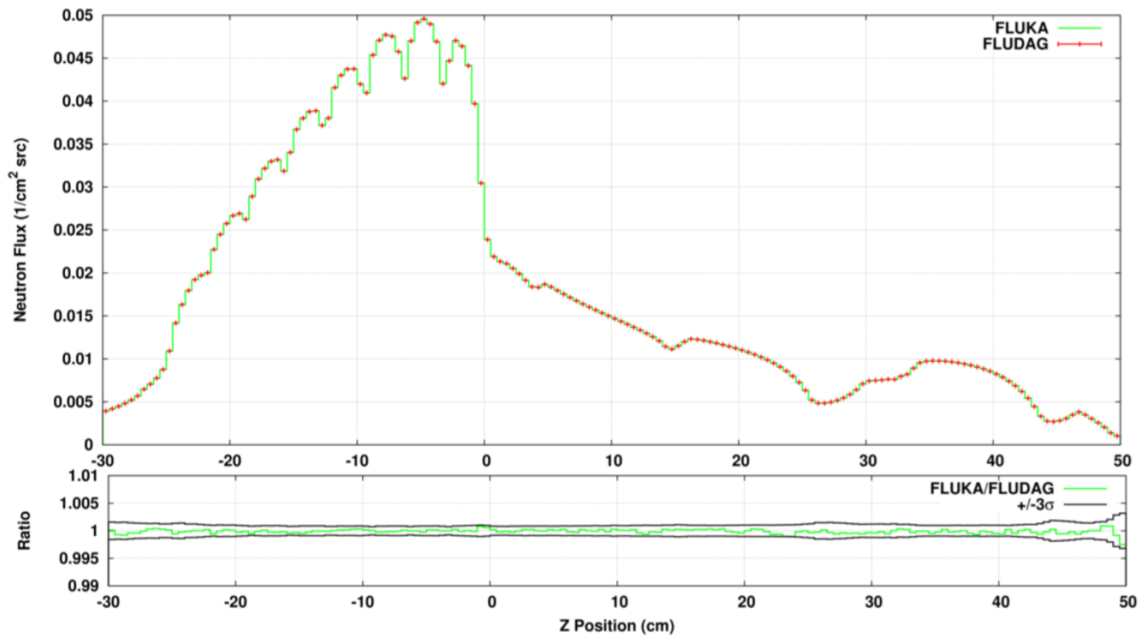


Figure 10: Neutron flux profiles, FLUKA as lines, FluDAG as points and the ratio of the profiles (FluDAG/Fluka)

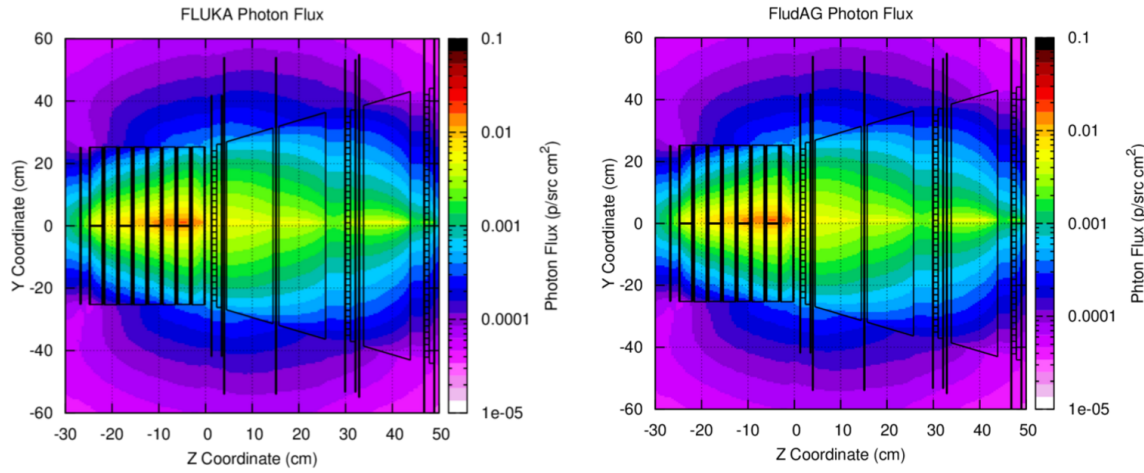


Figure 11: Photon flux profile determine in the native FLUKA geometry (left) and the FluDAG geometry (right)

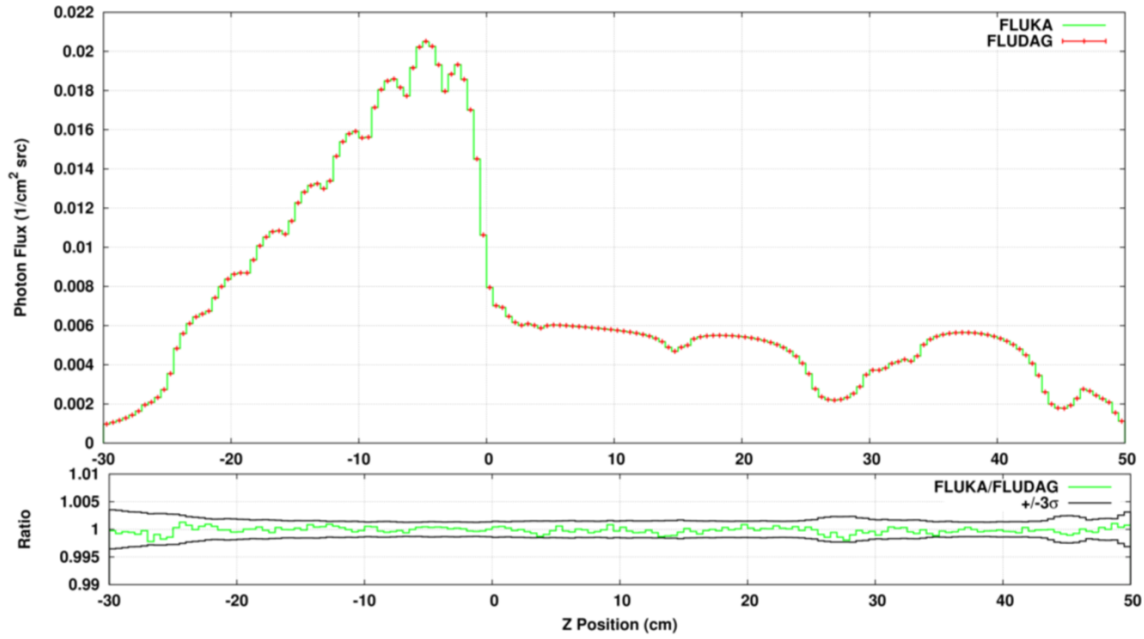


Figure 12: Photon flux profiles, FLUKA as lines, FluDAG as points and the ratio of the profiles (FluDAG/Fluka)

5.1.1 Conclusion

The results shown in the previous section were shown to give excellent agreement between Fluka & FluDAG. For all the particles examined there was agreement within the statistical errors with no outliers beyond 3σ . This along with other more simplistic benchmarking activities showed that there is a direct agreement between Fluka & FluDAG when equivalent geometries are used. Thus this work was presented at the 2014 Fluka Collaboration meeting and it was agreed that this work showed sufficient merit to consider doing further benchmarking as determined by the Fluka team.

5.1.2 AlAuAl

The AlAuAl (aluminium-gold-aluminium) benchmark originated from the development of FLUGG. The benchmark is specifically designed to stress electron transport in very thin layers. The geometry of the setup is shown in Figure 13.

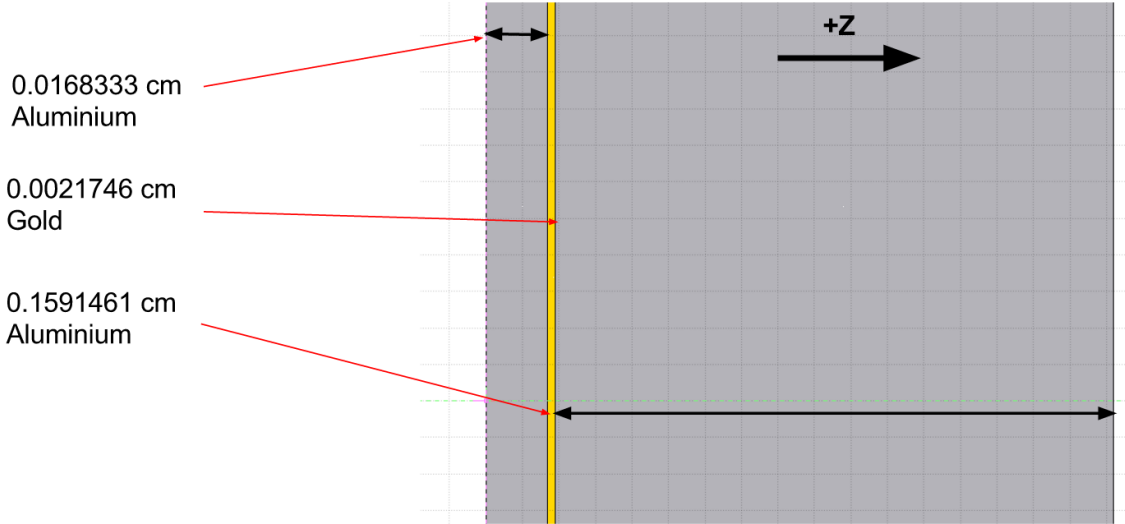


Figure 13: The geometry of the setup for the AlAuAl benchmark (FLUKA geometry shown)

The source is a 1 MeV pencil electron beam pointed in the positive z direction, with particles starting at 0,0,-10.0 cm. The CAD model for the FluDAG was created by exporting the native FLUKA geometry to MCNP format, then using mcnp2cad [ref] the CAD model was created. Each calculation was run with 5.0×10^5 with 20 batches.

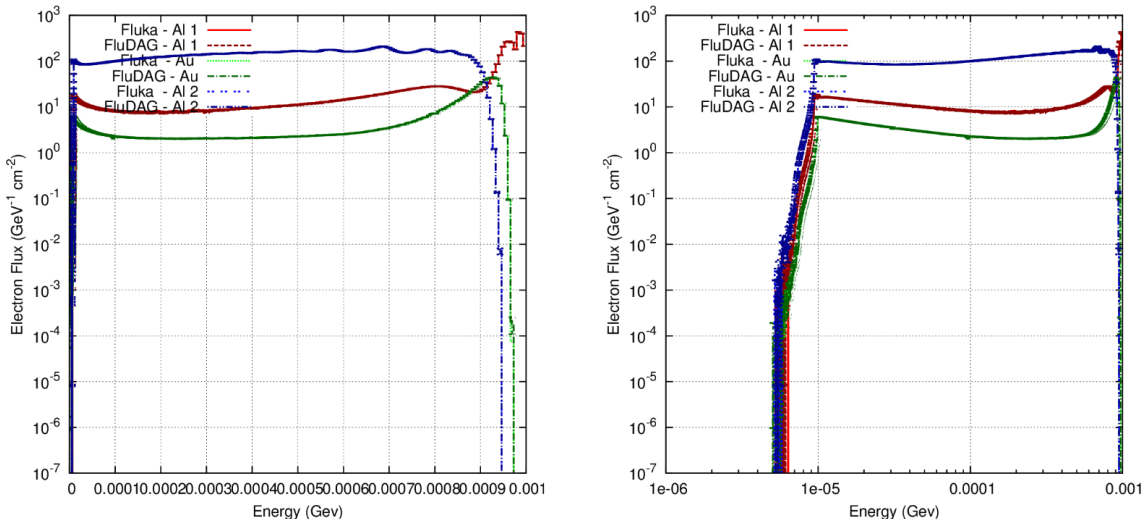


Figure 14

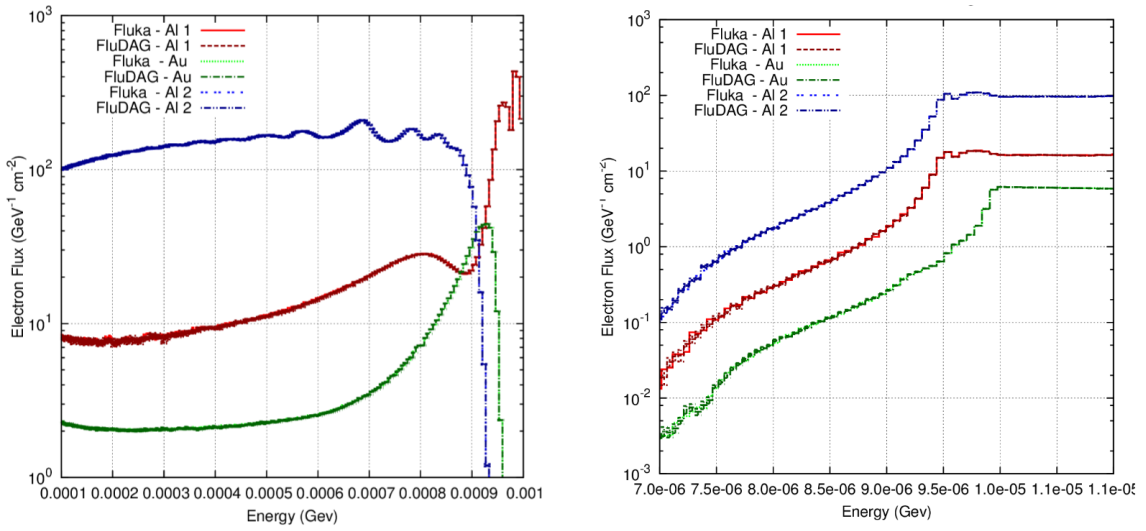


Figure 15

The suite of results displayed were shown to the FLUKA team at CERN during the FLUKA collaboration meeting in 2015, it was agreed then that the co-operation between the the results are excellent and show no artifacts in the transport of electrons.

5.1.3 Magnetic Field & Spheres

During the development of FLUGG a specific test case gave particularly pathogenic behaviour for electrons crossing boundaries between cells, the test is subsequently known as MagnSph and the geometry is shown in Figure 16. This test is particularly pathogenic for electron transport due to some of the peculiarities of electron transport in general and some of the FLUKA specific steps for electrons that are different than other particles. The true geometry is composed of cylinders and spheres which numerically touch.

It is not possible to represent the true geometry of this benchmark in CAD since it is not possible to resolve numerically touching, specifically with the Cubit based workflow, ACIS can only distinguish vertices as being distinct entities when they are greater than $1e-6$ cm apart. In this instance we found that the problem as originally defined resulted in several imprint and merge issues. Reducing the radii of cylinder from 0.5 to 0.49999 and the radii of the spheres from 0.3 to 0.29999 resulted in no issues regarding imprinting or merging. However, changing the radii to 0.499999 and 0.299999 respectively had the same issues as the unmodified model. Thus, the final model used for the benchmark calculations were has radii of cylinders and spheres of 0.49999 and 0.29999 respectively.

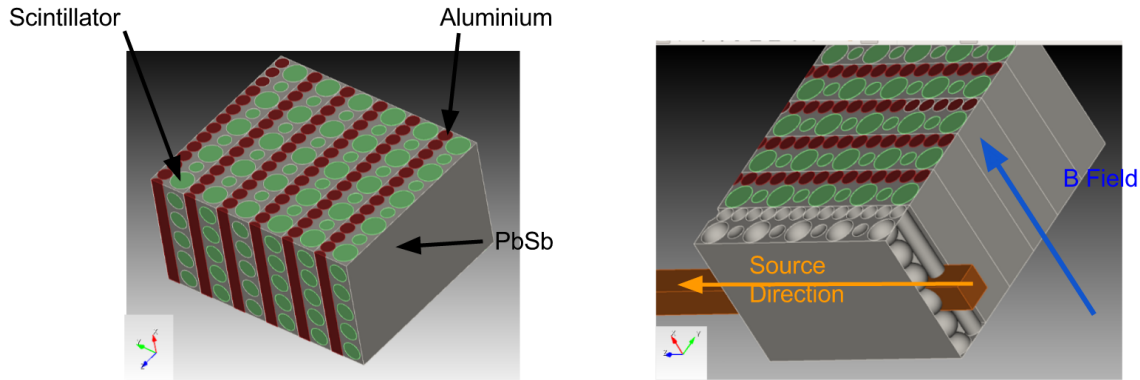


Figure 16: Geometry of the MagNSphe benchmark showing the incident positron source

The source is a square cross sectioned beam of side 1 cm containing positrons at 1 GeV, starting at $2,4,-1$ cm directed into the positive z direction. There is a uniform magnetic field of 60 T directed along the x direction.

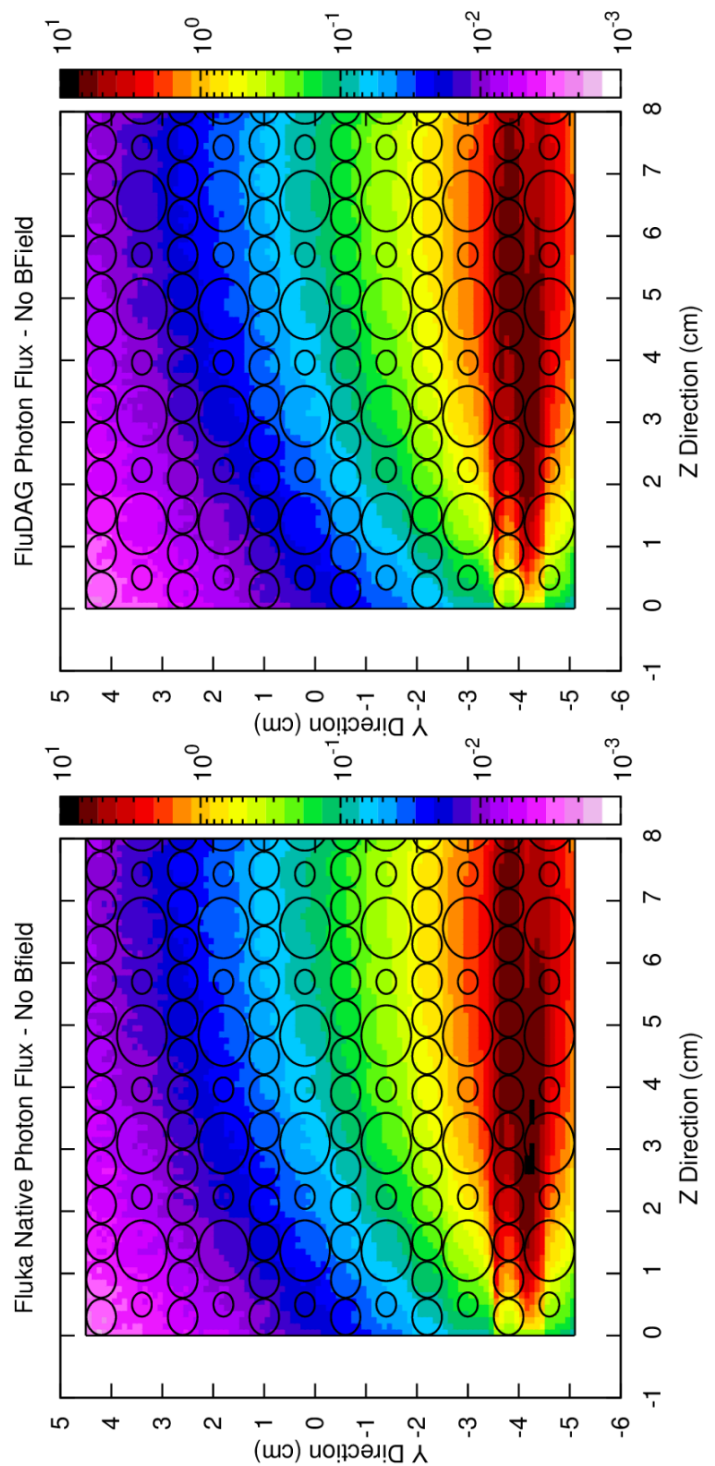


Figure 17: Photon flux determined in the Fluka (left) & FluDAG (right) in the case without magnetic field

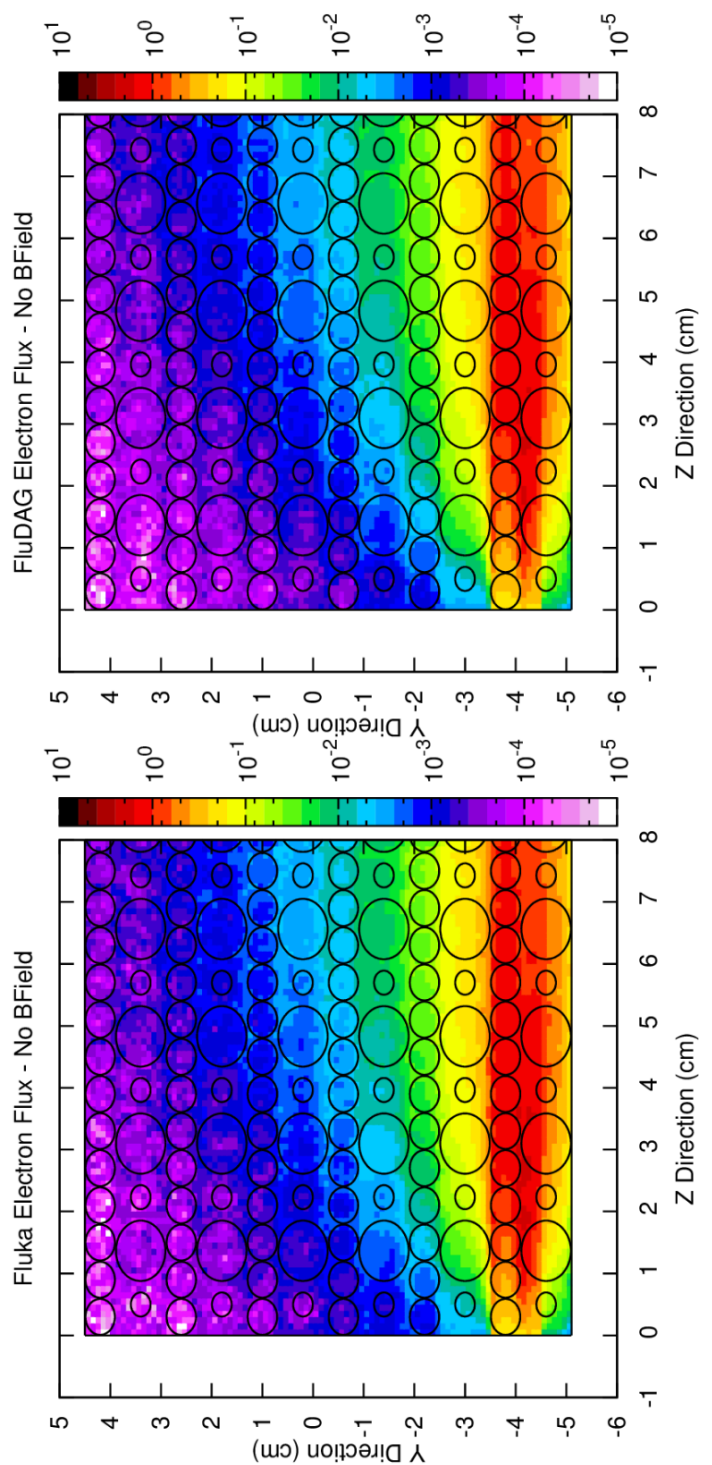


Figure 18: Electron flux determined in the Fluka (left) & FluDAG (right) in the case without magnetic field

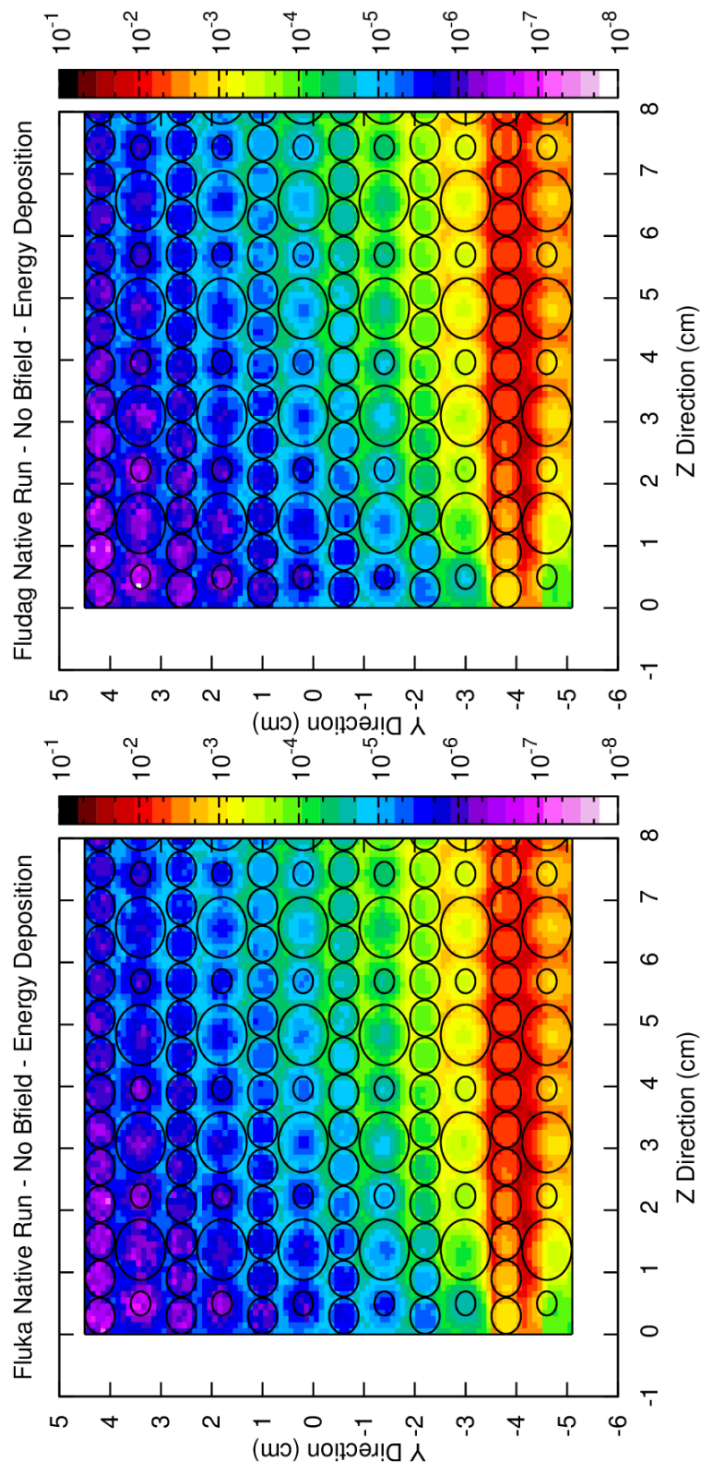


Figure 19: Energy deposition determined in the Fluka (left) & FluDAG (right) in the case without magnetic field

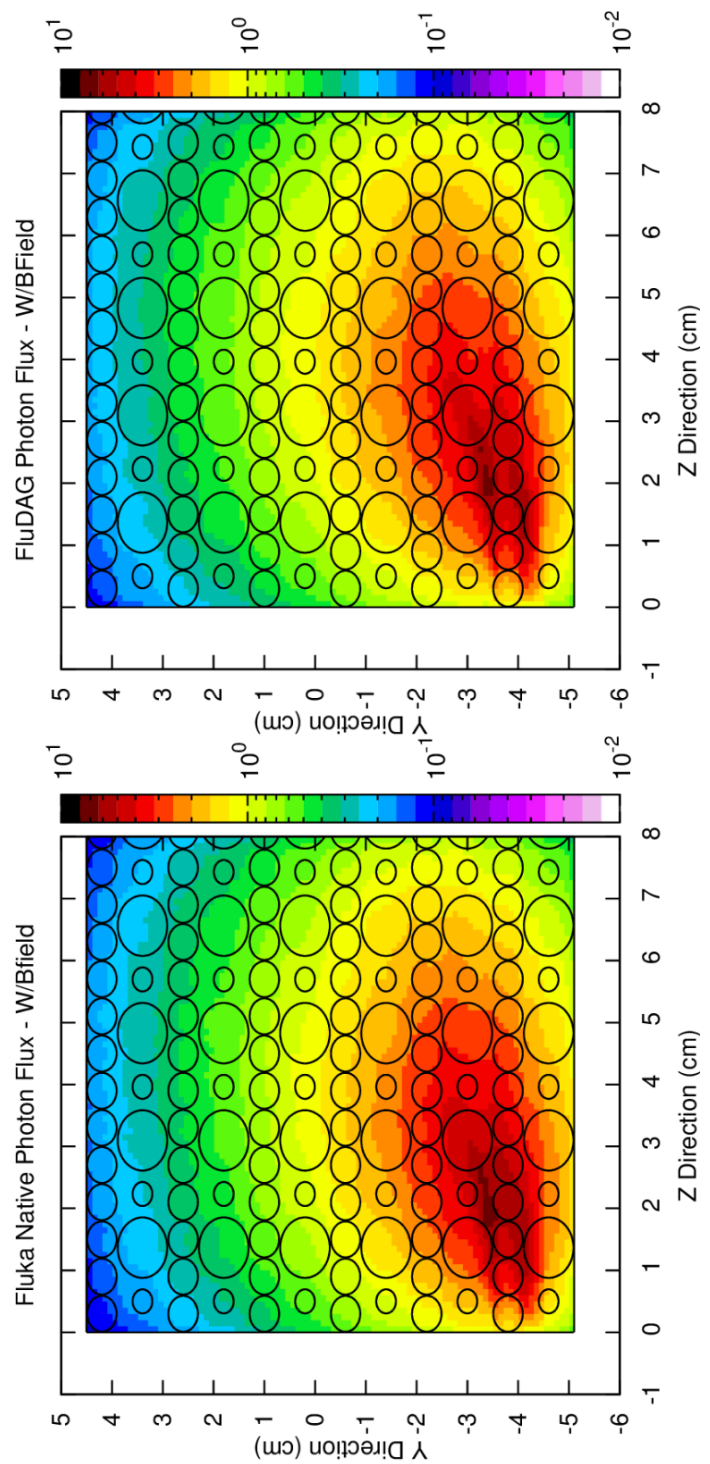


Figure 20: Photon flux determined in the Fluka (left) & FluDAG (right) in the case with magnetic fields

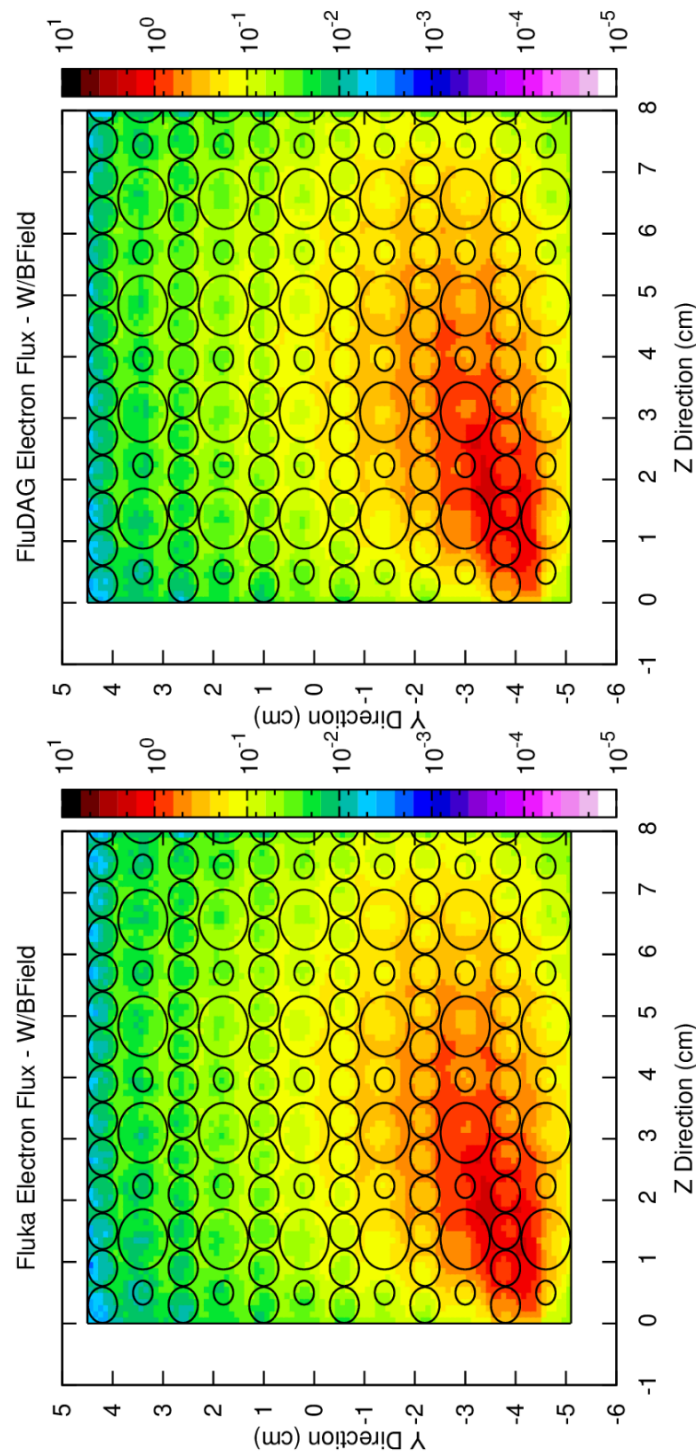


Figure 21: Electron flux determined in the Fluka (left) & FluDAG (right) in the case with magnetic fields

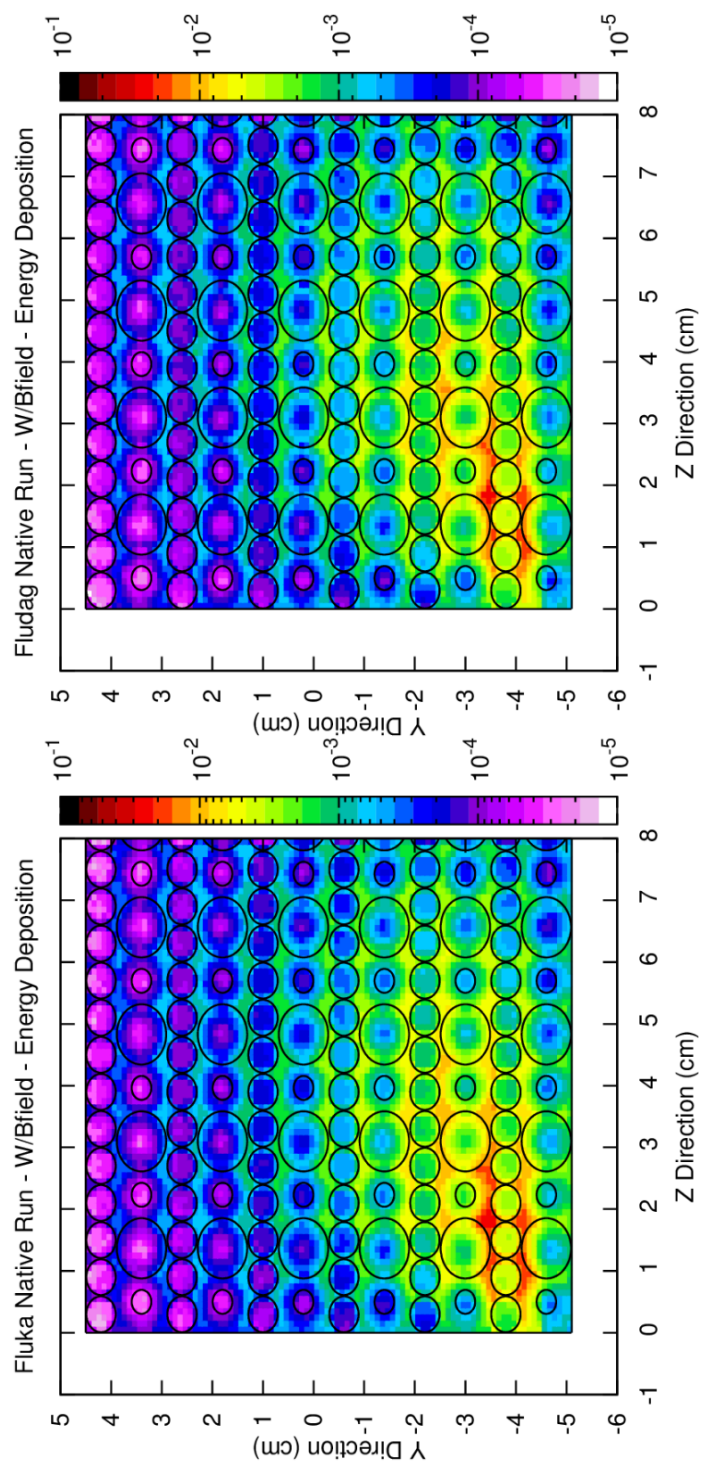


Figure 22: Energy deposition determined in the Fluka (left) & FluDAG (right) in the case with magnetic fields

6 Analysis

6.1 Mars Benchmarks

The purpose of this benchmark calculation was to demonstrate native FLUKA's ability to simulate the behavior of the Galactic Cosmic Ray (GCR) on the surface of Mars, and the fidelity with which we can calculate the dose received at the surface of Mars. The GCR source code is described in Section 4.4 , and the geometry of Mars will be described below.

6.1.1 Geometry

The geometry used in this benchmark calculation consisted of the surface of Mars and its atmosphere. To generate the geometry of mars, spherical shells were used. The first sphere modeled the planet and the rest of the spheres modeled the atmospheres. A region of interest was also defined in the geometry and this was 20 km by 20 km by 20 km in the x, y and z direction respectively where 0 height corresponds to the martian surface. The surface of the planet was made of Regolith with composition described in Appendix A. The atmosphere model consisted of layers of atmosphere with composition described in Appendix A and densities described by the following equation:

$$\rho = \rho_0 * \exp\left(-\frac{z}{H}\right) \quad (1)$$

Where z is the height at which we want the density, H is the scale height of the atmosphere, and $\rho_0 = 2E - 5g/cm^3$. A script was written in python to write input files that had different number of atmospheric layers, with its respective average density.

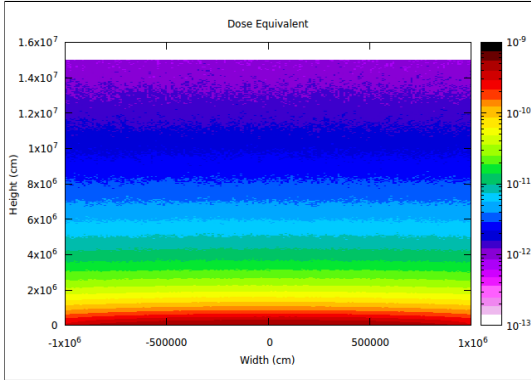
Several models were created and a benchmark calculation was performed in each of them. This was done with the purpose of understanding if the number of atmosphere layers significantly changed the dose at the surface of Mars and with what fidelity should the model be constructed.

A model with 27 and 146 atmospheric layers were first generated and results were compared (See results below). Because the results of the benchmark calculation run with the models described above did not show significant difference, the final model consisted of 20 layers of atmosphere. This was done as specified by NASA's atmosphere model given in Appendix A.

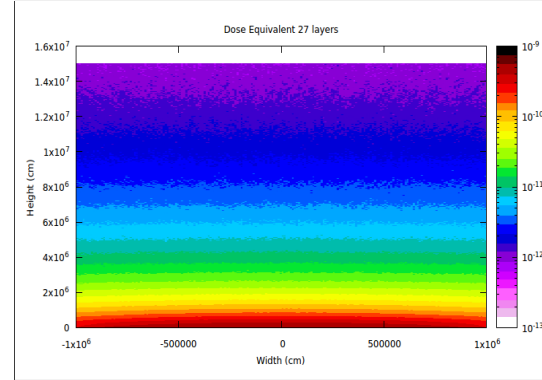
This 20 layer model was presented at the Colorado conference. This model was run a little different than the previous two models. In this case, the tallies were used were dose in the first layer and last layers as well as proton, neutron and deuteron fluxes. This model was also biased by isotope from $z = 1$ to $z = 28$ to help sample each isotope better. The final results of each isotope run was collected together to have one final dose. This was done with the help of a script created by NASA.

6.1.2 Workflow

The input file was created in native FLUKA where the source, the geometry specified above, the number of primaries, the tallies wanted, and any other specification were provided. The model was then run in a High Throughput Computing system with the aid of a CHTC tools work flow.



(a) 146 layers model



(b) 27 layers model

Figure 23: Dose Deposition

6.1.3 Results

Figure 23a shows the dose throughout the atmosphere for 146 layers model and figure 23b shows the dose for the 27 layers model.

The neutron flux was also calculated and compared between the two models. The differences between them were insignificant. Figure 24 shows the neutron flux from the surface to the first atmosphere and vice-versa.

The results for the 20 layers models was collected for all isotopes and assembled together by NASA. Some results for individual isotopes will be presented below. Figure 25 shows the flux at the surface of Mars for proton biased source.

6.1.4 Conclusion

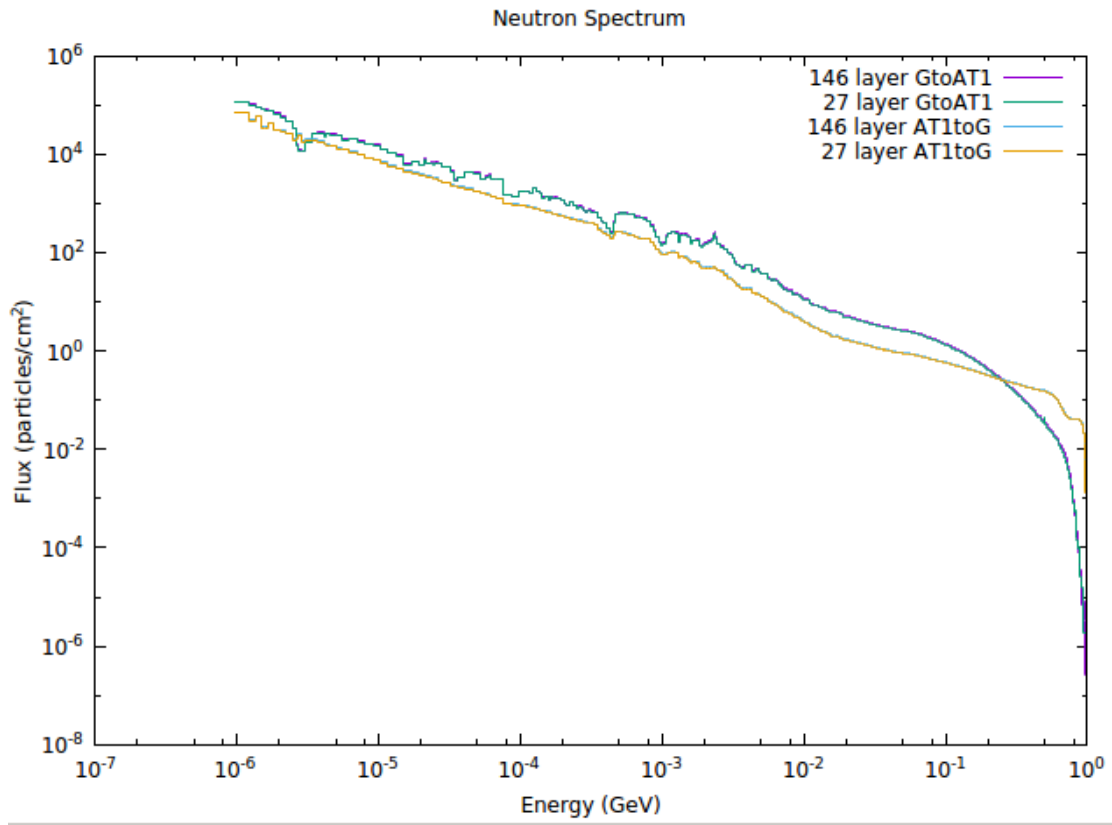


Figure 24: Neutron flux for 27 layer and 146 layer model

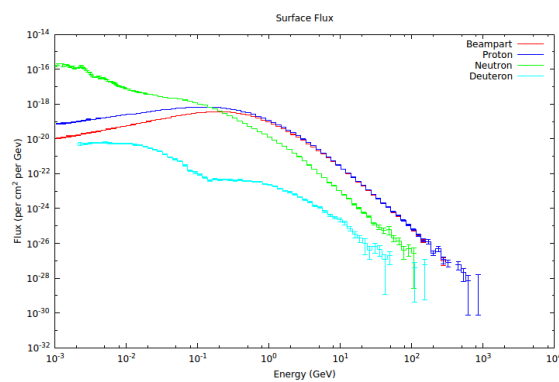


Figure 25: Flux at the surface of Mars for proton biased source

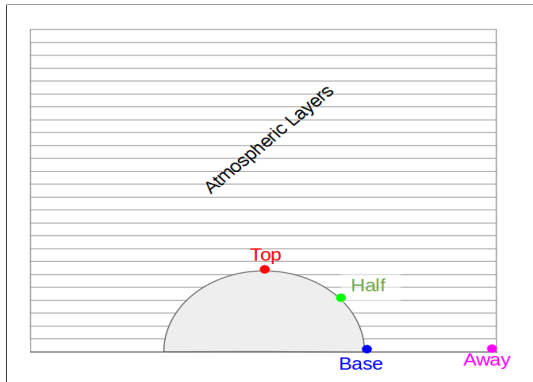
6.2 Topology Calculations

In an effort to provide better fidelity of the mars topology, a benchmark calculation was designed that consisted of adding mountains and craters to the Mars surface. The input files were created in FLUKA and run similarly to the benchmark calculations for the atmospheres.

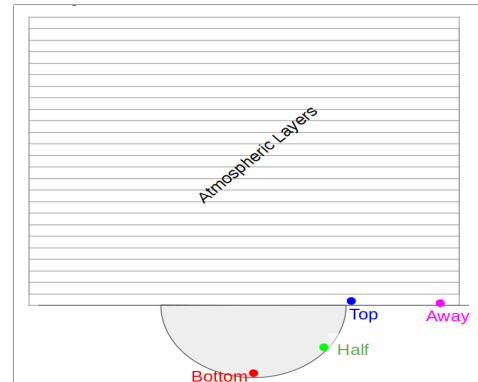
Geometry

The mountains were created on the surface of Mars and were designed to be 5 km high and 10 km wide, whereas the craters were designed to be 5 km deep and 10 km wide. Variations of the mountain and crater described above were modeled. Nine different models were created for mountains and nine for craters. These variations were 1/3, 2/3 and 3/3 of the height with base of 1/3, 2/3 and 3/3.

In the interest of calculating dose, detectors were set at the top, half way up, base, and away from the mountain. The crater had similar detectors. A schematics of the set up can be seen in figure 26a for mountains and figure 26b for craters.



(a) Mountain



(b) Crater

Figure 26: Geometry set up with detectors and atmospheric layers

Results

A mountain and a crater with base of 10 km and height or depth of 5 km were used to obtain the following results.

For the first calculation tallies for energy deposition were set and the results can be seen in figure 27 for mountains and in figure 28 for craters.

The total response at each of the detectors was also calculated for several particles of interest. The results can be seen in figure 29a and 29b.

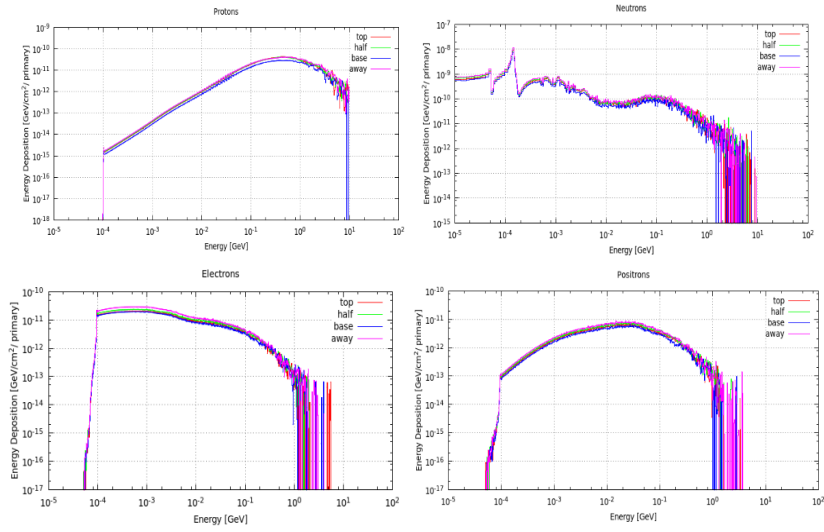


Figure 27: Energy deposition in the mountain for protons, neutrons, electrons and positrons

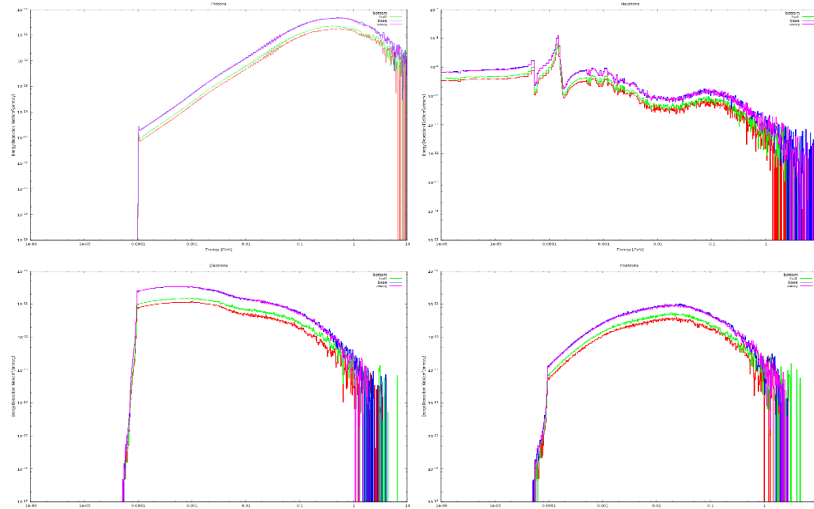


Figure 28: Energy deposition in the crater for protons, neutrons, electrons and positrons

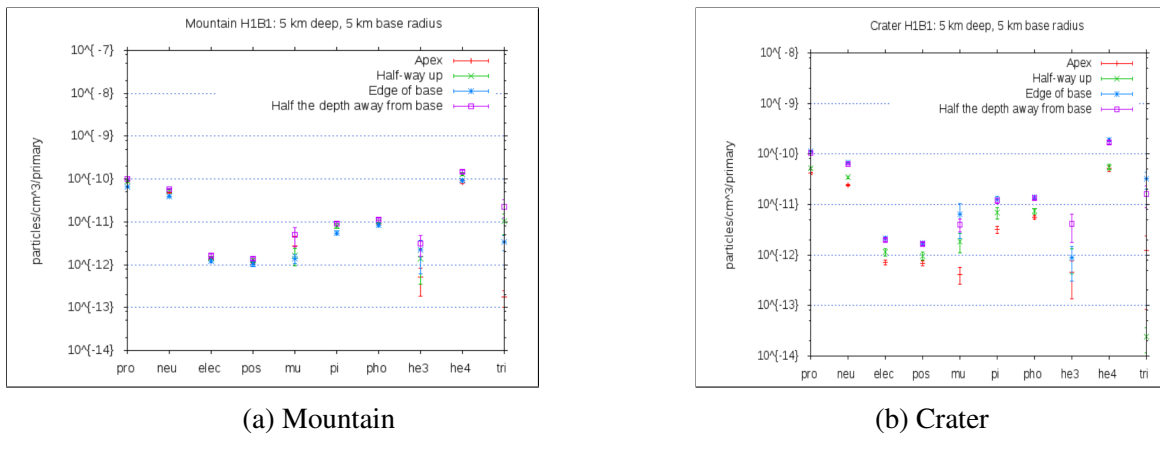


Figure 29: Total response at each detector

6.3 Phantom in Mars Habitat Module

The purpose of this calculation was to demonstrate the ability to simulate a detailed human phantom inside a habitat module in the radiation environment that exists on the surface of Mars. Some of the challenges included finding a high fidelity human phantom suitable for radiation transport, composing the full geometry from components generated by different methods, and accurately simulating the GCR spectrum and applying it such that a fair number of particles would reach the regions of interest. Proof of this capability is a necessary first step in the ultimate goal of calculating cancer risk to astronauts in future Mars missions.

Geometry

The human phantom geometry was generated by a medical physics group at the University of Florida. First, a voxel model of the phantom was created from CT scan data. The voxel model was used to generate a Wavefront OBJ file and ReadOBJ was then used to convert the OBJ file to an HDF5 file.

A CAD model of the habitat module was created by NASA and the ACIS file was imported into Trelis. The DAGMC Trelis plugin was used to export a faceted version of the file.

As a first approximation, Mars was represented by a 1200 m x 1200 m x 10 m block of regolith. The CAD model of the planet was created with Trelis and the faceted, file was exported. In the future, it could be found that topological features of the planet make a significant difference in dose received by the human inside the habitat module. In this case, a more detailed model of the planet will need to be used.

In this particular calculation, the atmosphere was not explicitly modeled by CAD geometry surfaces due to the complicated boolean subtraction of surfaces that would need to occur between the atmosphere and the habitat module. Instead, the atmosphere was accounted for by giving the implicit compliment the composition and density of the atmospheric layer closest to the surface of Mars.

Workflow

HDF5 files of the phantom, habitat, and regolith were combined into a single geometry file using the combine_geoms tool. The material compositions given in Appendix A were used to generate a material library using the PyNE Material class. Each object in the geometry was tagged with a material. The materials and tallies were then applied to the geometry file via uwuw_preproc. Specifically, a NASA/Cancer-Risk tally was applied to all phantom objects that have the tally tag. Mainfludag was then used to generate the materials and cancer-risk scoring sections of the FLUKA input file. Global mesh scoring for total energy deposition was also added to the input file. The source used was the full GCR spectrum as detailed in previous sections.

Results

For proof of concept, a short FluDAG calculation with 1e4 histories was run on a desktop machine. Because so few histories were run, the cancer risk scoring in each phantom region did not yield any useful results. Many more histories will need to be run with the use of a computing cluster in order to achieve statistically accurate results. The results from the global mesh scoring of energy deposition are shown below. This successfully demonstrates the ability of a problem of this scale to be run.

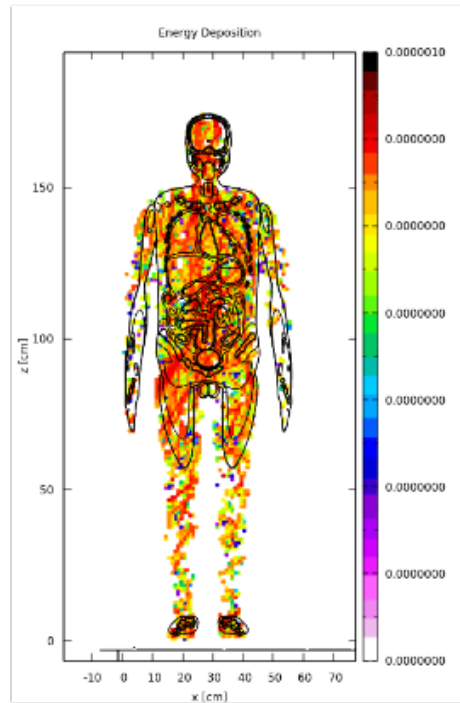


Figure 30: Energy deposition in phantom

References

- [1] T. J. Tautges, P. P. H. Wilson, J. Kraftcheck, B. M. Smith, and D. L. Henderson, “Acceleration techniques for direct use of CAD-Based geometries in monte carlo radiation transport,” in *Int'l Conf. on Mathematics, Computational Methods & Reactor Physics (M&C 2009)*, (Saratoga Springs, NY), American Nuclear Society, May 2009.
- [2] T. J. Tautges, R. Meyers, K. Merkley, C. Stimpson, and C. Ernst, “MOAB: a mesh-oriented database,” SAND2004-1592, Sandia National Laboratories, Apr. 2004.
- [3] G. Battistoni, F. Cerutti, A. Fasso, A. Ferrari, S. Muraro, J. Ranft, S. Roesler, and P. R. Sala, “The FLUKA code: description and benchmarking,” *AIP Conference Proceedings*, vol. 896, pp. 31–49, Mar. 2007.
- [4] M. Campanella, A. Ferrari, P. Sala, and S. Vanini, “Reusing code from FLUKA and GEANT4 geometry,” Tech. Rep. ATL-SOFT-98-039, Oct. 1998.
- [5] S. Agostinelli, J. Allison, K. Amako, J. Apostolakis, H. Araujo, P. Arce, M. Asai, D. Axen, S. Banerjee, G. Barrand, F. Behner, L. Bellagamba, J. Boudreau, L. Broglia, A. Brunengo, H. Burkhardt, S. Chauvie, J. Chuma, R. Chytracek, G. Cooperman, G. Cosmo, P. Degtyarenko, A. Dell'Acqua, G. Depaola, D. Dietrich, R. Enami, A. Feliciello, C. Ferguson, H. Fesefeldt, G. Folger, F. Foppiano, A. Forti, S. Garelli, S. Giani, R. Giannitrapani, D. Gibin, J. Gmez Cadenas, I. Gonzlez, G. Gracia Abril, G. Greeniaus, W. Greiner, V. Grichine, A. Grossheim, S. Guatelli, P. Gumplinger, R. Hamatsu, K. Hashimoto, H. Hasui, A. Heikkinen, A. Howard, V. Ivanchenko, A. Johnson, F. Jones, J. Kallenbach, N. Kanaya, M. Kawabata, Y. Kawabata, M. Kawaguti, S. Kelner, P. Kent, A. Kimura, T. Kodama, R. Kokoulin, M. Kossov, H. Kurashige, E. Lamanna, T. Lampn, V. Lara, V. Lefebure, F. Lei, M. Liendl, W. Lockman, F. Longo, S. Magni, M. Maire, E. Medernach, K. Minamimoto, P. Mora de Freitas, Y. Morita, K. Murakami, M. Nagamatu, R. Nartallo, P. Nieminen, T. Nishimura, K. Ohtsubo, M. Okamura, S. O'Neale, Y. Oohata, K. Paech, J. Perl, A. Pfeiffer, M. Pia, F. Ranjard, A. Rybin, S. Sadilov, E. Di Salvo, G. Santin, T. Sasaki, N. Savvas, Y. Sawada, S. Scherer, S. Sei, V. Sirotenko, D. Smith, N. Starkov, H. Stoecker, J. Sulkimo, M. Takahata, S. Tanaka, E. Tcherniaev, E. Safai Tehrani, M. Tropeano, P. Truscott, H. Uno, L. Urban, P. Urban, M. Verderi, A. Walkden, W. Wander, H. Weber, J. Wellisch, T. Wenaus, D. Williams, D. Wright, T. Yamada, H. Yoshida, and D. Zschiesche, “Geant4-a simulation toolkit,” *Nuclear Inst. & Methods in Phys. Res. Section A: Accel., Spectrometers, Detectors and Associated Equipment*, vol. 506, pp. 250–303, July 2003.
- [6] M. C. Han, C. H. Kim, J. H. Jeong, Y. S. Yeom, S. Kim, P. P. H. Wilson, and J. Apostolakis, “DagSolid: a new geant4 solid class for fast simulation in polygon-mesh geometry,” *Physics in Medicine and Biology*, vol. 58, p. 4595, July 2013.

A Materials

Material	Nuclide	Mass Fraction
Subcutaneous_Fat		
	H1	1.13774e+01
	H2	2.61509e-03
	C12	5.81781e+01
	C13	6.81852e-01
	N14	7.47076e-01
	N15	2.92362e-03
	O16	2.86222e+01
	O17	1.15875e-02
	O18	6.61887e-02
	Na23	1.00000e-01
	P31	1.00000e-01
	S32	9.47153e-02
	S33	7.71207e-04
	S34	4.50224e-03
	S36	1.12170e-05
	Cl35	7.47256e-03
	Cl37	2.52744e-03
Muscle		
	H1	1.01977e+01
	H2	2.34393e-03
	C12	1.40652e+01
	C13	1.64845e-01
	N14	3.38675e+00
	N15	1.32538e-02
	O16	7.08774e+01
	O17	2.86941e-02
	O18	1.63904e-01
	Na23	1.00000e-01
	P31	2.00000e-01
	S32	2.84146e-01
	S33	2.31362e-03
	S34	1.35067e-02
	S36	3.36510e-05
	Cl35	7.47256e-02
	Cl37	2.52744e-02
	K39	3.71748e-01
	K40	4.78362e-05
	K41	2.82039e-02

Visceral_Fat	
H1	1.13774e+01
H2	2.61509e-03
C12	5.81781e+01
C13	6.81852e-01
N14	7.47076e-01
N15	2.92362e-03
O16	2.86222e+01
O17	1.15875e-02
O18	6.61887e-02
Na23	1.00000e-01
P31	1.00000e-01
S32	9.47153e-02
S33	7.71207e-04
S34	4.50224e-03
S36	1.12170e-05
Cl35	7.47256e-03
Cl37	2.52744e-03
Blood	
H1	1.01977e+01
H2	2.34393e-03
C12	1.08726e+01
C13	1.27427e-01
N14	3.28714e+00
N15	1.28639e-02
O16	7.42981e+01
O17	3.00790e-02
O18	1.71814e-01
Na23	1.00000e-01
P31	1.00000e-01
S32	1.89431e-01
S33	1.54241e-03
S34	9.00448e-03
S36	2.24340e-05
Cl35	2.24177e-01
Cl37	7.58233e-02
K39	1.85874e-01
K40	2.39181e-05
K41	1.41020e-02
Fe54	5.64556e-03
Fe56	9.19015e-02
Fe57	2.16037e-03

	Fe58	2.92544e-04
Soft_Tissue_M		
H1	1.04976e+01	
H2	2.41287e-03	
C12	2.53034e+01	
C13	2.96558e-01	
N14	2.68947e+00	
N15	1.05250e-02	
O16	6.00369e+01	
O17	2.43054e-02	
O18	1.38835e-01	
Na23	1.00000e-01	
P31	2.00000e-01	
S32	2.84146e-01	
S33	2.31362e-03	
S34	1.35067e-02	
S36	3.36510e-05	
Cl35	1.49451e-01	
Cl37	5.05489e-02	
K39	1.85874e-01	
K40	2.39181e-05	
K41	1.41020e-02	
Soft_Tissue_F		
H1	1.05976e+01	
H2	2.43585e-03	
C12	3.11351e+01	
C13	3.64905e-01	
N14	2.39064e+00	
N15	9.35559e-03	
O16	5.45518e+01	
O17	2.20848e-02	
O18	1.26151e-01	
Na23	1.00000e-01	
P31	2.00000e-01	
S32	1.89431e-01	
S33	1.54241e-03	
S34	9.00448e-03	
S36	2.24340e-05	
Cl35	7.47256e-02	
Cl37	2.52744e-02	
K39	1.85874e-01	
K40	2.39181e-05	

	K41	1.41020e-02
Skin		
H1	1.00077e+01	
H2	2.30027e-03	
C12	1.97387e+01	
C13	2.31338e-01	
N14	4.14378e+00	
N15	1.62164e-02	
O16	6.47840e+01	
O17	2.62272e-02	
O18	1.49813e-01	
Na23	2.00000e-01	
P31	1.00000e-01	
S32	1.89431e-01	
S33	1.54241e-03	
S34	9.00448e-03	
S36	2.24340e-05	
Cl35	2.24177e-01	
Cl37	7.58233e-02	
K39	9.29371e-02	
K40	1.19591e-05	
K41	7.05098e-03	
Lymph_Nodes		
H1	1.04776e+01	
H2	2.40827e-03	
C12	2.45325e+01	
C13	2.87522e-01	
N14	2.71936e+00	
N15	1.06420e-02	
O16	6.07948e+01	
O17	2.46123e-02	
O18	1.40588e-01	
Na23	1.00000e-01	
P31	1.90000e-01	
S32	2.74674e-01	
S33	2.23650e-03	
S34	1.30565e-02	
S36	3.25293e-05	
Cl35	1.56924e-01	
Cl37	5.30763e-02	
K39	1.85874e-01	
K40	2.39181e-05	

K41	1.41020e-02
Fe54	5.64556e-04
Fe56	9.19015e-03
Fe57	2.16037e-04
Fe58	2.92544e-05
Air	
C12	9.88416e-03
C13	1.15843e-04
N14	7.52356e+01
N15	2.94428e-01
O16	2.31172e+01
O17	9.35880e-03
O18	5.34584e-02
Ar36	3.84462e-03
Ar38	7.65112e-04
Ar40	1.27539e+00
Water	
H1	1.11974e+01
H2	2.57373e-03
O16	8.85594e+01
O17	3.58525e-02
O18	2.04793e-01
Carbon	
C12	9.88416e+01
C13	1.15843e+00
Brain	
H1	1.06775e+01
H2	2.45423e-03
C12	1.41739e+01
C13	1.66119e-01
N14	2.24123e+00
N15	8.77086e-03
O16	7.11566e+01
O17	2.88072e-02
O18	1.64549e-01
Na23	2.00000e-01
P31	3.90000e-01
S32	1.89431e-01
S33	1.54241e-03
S34	9.00448e-03
S36	2.24340e-05
Cl35	2.24177e-01

Cl37	7.58233e-02
K39	2.78811e-01
K40	3.58772e-05
K41	2.11529e-02
<hr/>	
Nasal Layer	
H1	1.04276e+01
H2	2.39678e-03
C12	2.21109e+01
C13	2.59141e-01
N14	2.81897e+00
N15	1.10318e-02
O16	6.31883e+01
O17	2.55812e-02
O18	1.46123e-01
Na23	1.00000e-01
P31	1.80000e-01
S32	2.65203e-01
S33	2.15938e-03
S34	1.26063e-02
S36	3.14076e-05
Cl35	1.64396e-01
Cl37	5.56038e-02
K39	1.85874e-01
K40	2.39181e-05
K41	1.41020e-02
Fe54	1.12911e-03
Fe56	1.83803e-02
Fe57	4.32074e-04
Fe58	5.85089e-05
<hr/>	
Eye	
H1	9.59779e+00
H2	2.20605e-03
C12	1.92741e+01
C13	2.25894e-01
N14	5.67778e+00
N15	2.22195e-02
O16	6.44249e+01
O17	2.60819e-02
O18	1.48982e-01
Na23	1.00000e-01
P31	1.00000e-01
S32	2.84146e-01

S33	2.31362e-03
S34	1.35067e-02
S36	3.36510e-05
Cl35	7.47256e-02
Cl37	2.52744e-02
<hr/>	
Lens	
H1	9.59779e+00
H2	2.20605e-03
C12	1.92741e+01
C13	2.25894e-01
N14	5.67778e+00
N15	2.22195e-02
O16	6.44249e+01
O17	2.60819e-02
O18	1.48982e-01
Na23	1.00000e-01
P31	1.00000e-01
S32	2.84146e-01
S33	2.31362e-03
S34	1.35067e-02
S36	3.36510e-05
Cl35	7.47256e-02
Cl37	2.52744e-02
<hr/>	
External_Nose	
H1	9.72776e+00
H2	2.23592e-03
C12	1.00225e+01
C13	1.17465e-01
N14	2.43049e+00
N15	9.51151e-03
O16	7.42183e+01
O17	3.00467e-02
O18	1.71629e-01
Na23	4.10000e-01
P31	1.74000e+00
S32	7.10365e-01
S33	5.78405e-03
S34	3.37668e-02
S36	8.41275e-05
Cl35	2.24177e-01
Cl37	7.58233e-02
K39	3.71748e-02

K40	4.78362e-06
K41	2.82039e-03
Fe54	1.12911e-03
Fe56	1.83803e-02
Fe57	4.32074e-04
Fe58	5.85089e-05
<hr/>	
Ears	
H1	9.72776e+00
H2	2.23592e-03
C12	1.00225e+01
C13	1.17465e-01
N14	2.43049e+00
N15	9.51151e-03
O16	7.42183e+01
O17	3.00467e-02
O18	1.71629e-01
Na23	4.10000e-01
P31	1.74000e+00
S32	7.10365e-01
S33	5.78405e-03
S34	3.37668e-02
S36	8.41275e-05
Cl35	2.24177e-01
Cl37	7.58233e-02
K39	3.71748e-02
K40	4.78362e-06
K41	2.82039e-03
Fe54	1.12911e-03
Fe56	1.83803e-02
Fe57	4.32074e-04
Fe58	5.85089e-05
<hr/>	
Pituitary_Gland	
H1	1.04276e+01
H2	2.39678e-03
C12	2.21109e+01
C13	2.59141e-01
N14	2.81897e+00
N15	1.10318e-02
O16	6.31883e+01
O17	2.55812e-02
O18	1.46123e-01
Na23	1.00000e-01

P31	1.80000e-01
S32	2.65203e-01
S33	2.15938e-03
S34	1.26063e-02
S36	3.14076e-05
Cl35	1.64396e-01
Cl37	5.56038e-02
K39	1.85874e-01
K40	2.39181e-05
K41	1.41020e-02
Fe54	1.12911e-03
Fe56	1.83803e-02
Fe57	4.32074e-04
Fe58	5.85089e-05
<hr/>	
Salivary_Glands	
H1	1.04276e+01
H2	2.39678e-03
C12	2.21109e+01
C13	2.59141e-01
N14	2.81897e+00
N15	1.10318e-02
O16	6.31883e+01
O17	2.55812e-02
O18	1.46123e-01
Na23	1.00000e-01
P31	1.80000e-01
S32	2.65203e-01
S33	2.15938e-03
S34	1.26063e-02
S36	3.14076e-05
Cl35	1.64396e-01
Cl37	5.56038e-02
K39	1.85874e-01
K40	2.39181e-05
K41	1.41020e-02
Fe54	1.12911e-03
Fe56	1.83803e-02
Fe57	4.32074e-04
Fe58	5.85089e-05
<hr/>	
Oral_Cavity_Layer	
H1	1.04276e+01
H2	2.39678e-03

C12	2.21109e+01
C13	2.59141e-01
N14	2.81897e+00
N15	1.10318e-02
O16	6.31883e+01
O17	2.55812e-02
O18	1.46123e-01
Na23	1.00000e-01
P31	1.80000e-01
S32	2.65203e-01
S33	2.15938e-03
S34	1.26063e-02
S36	3.14076e-05
Cl35	1.64396e-01
Cl37	5.56038e-02
K39	1.85874e-01
K40	2.39181e-05
K41	1.41020e-02
Fe54	1.12911e-03
Fe56	1.83803e-02
Fe57	4.32074e-04
Fe58	5.85089e-05

Tongue	
H1	1.01977e+01
H2	2.34393e-03
C12	1.34128e+01
C13	1.57199e-01
N14	3.36682e+00
N15	1.31758e-02
O16	7.15755e+01
O17	2.89767e-02
O18	1.65518e-01
Na23	1.00000e-01
P31	1.80000e-01
S32	2.65203e-01
S33	2.15938e-03
S34	1.26063e-02
S36	3.14076e-05
Cl35	1.04616e-01
Cl37	3.53842e-02
K39	3.34573e-01
K40	4.30526e-05

K41	2.53835e-02
Fe54	1.12911e-03
Fe56	1.83803e-02
Fe57	4.32074e-04
Fe58	5.85089e-05
<hr/>	
Tonsils	
H1	1.04276e+01
H2	2.39678e-03
C12	2.21109e+01
C13	2.59141e-01
N14	2.81897e+00
N15	1.10318e-02
O16	6.31883e+01
O17	2.55812e-02
O18	1.46123e-01
Na23	1.00000e-01
P31	1.80000e-01
S32	2.65203e-01
S33	2.15938e-03
S34	1.26063e-02
S36	3.14076e-05
Cl35	1.64396e-01
Cl37	5.56038e-02
K39	1.85874e-01
K40	2.39181e-05
K41	1.41020e-02
Fe54	1.12911e-03
Fe56	1.83803e-02
Fe57	4.32074e-04
Fe58	5.85089e-05
<hr/>	
Pharynx	
H1	1.04276e+01
H2	2.39678e-03
C12	2.21109e+01
C13	2.59141e-01
N14	2.81897e+00
N15	1.10318e-02
O16	6.31883e+01
O17	2.55812e-02
O18	1.46123e-01
Na23	1.00000e-01
P31	1.80000e-01

S32	2.65203e-01
S33	2.15938e-03
S34	1.26063e-02
S36	3.14076e-05
Cl35	1.64396e-01
Cl37	5.56038e-02
K39	1.85874e-01
K40	2.39181e-05
K41	1.41020e-02
Fe54	1.12911e-03
Fe56	1.83803e-02
Fe57	4.32074e-04
Fe58	5.85089e-05
<hr/>	
Spinal_Cord	
H1	1.05876e+01
H2	2.43355e-03
C12	1.35709e+01
C13	1.59052e-01
N14	2.43049e+00
N15	9.51151e-03
O16	7.17351e+01
O17	2.90413e-02
O18	1.65887e-01
Na23	1.80000e-01
P31	3.30000e-01
S32	1.89431e-01
S33	1.54241e-03
S34	9.00448e-03
S36	2.24340e-05
Cl35	2.24177e-01
Cl37	7.58233e-02
K39	2.60224e-01
K40	3.34854e-05
K41	1.97427e-02
Fe54	1.12911e-03
Fe56	1.83803e-02
Fe57	4.32074e-04
Fe58	5.85089e-05
<hr/>	
Larynx	
H1	9.72776e+00
H2	2.23592e-03
C12	1.00225e+01

C13	1.17465e-01
N14	2.43049e+00
N15	9.51151e-03
O16	7.42183e+01
O17	3.00467e-02
O18	1.71629e-01
Na23	4.10000e-01
P31	1.74000e+00
S32	7.10365e-01
S33	5.78405e-03
S34	3.37668e-02
S36	8.41275e-05
Cl35	2.24177e-01
Cl37	7.58233e-02
K39	3.71748e-02
K40	4.78362e-06
K41	2.82039e-03
Fe54	1.12911e-03
Fe56	1.83803e-02
Fe57	4.32074e-04
Fe58	5.85089e-05

Thyroid

H1	1.03676e+01
H2	2.38299e-03
C12	1.16139e+01
C13	1.36115e-01
N14	2.54006e+00
N15	9.94031e-03
O16	7.42981e+01
O17	3.00790e-02
O18	1.71814e-01
Na23	1.80000e-01
P31	1.00000e-01
S32	1.13658e-01
S33	9.25449e-04
S34	5.40269e-03
S36	1.34604e-05
Cl35	1.64396e-01
Cl37	5.56038e-02
K39	1.11524e-01
K40	1.43509e-05
K41	8.46117e-03

Fe54	1.12911e-03
Fe56	1.83803e-02
Fe57	4.32074e-04
Fe58	5.85089e-05
I127	8.00000e-02
<hr/>	
Esophagus	
H1	1.04076e+01
H2	2.39219e-03
C12	2.10533e+01
C13	2.46745e-01
N14	2.86877e+00
N15	1.12267e-02
O16	6.42355e+01
O17	2.60052e-02
O18	1.48544e-01
Na23	1.00000e-01
P31	1.70000e-01
S32	2.55731e-01
S33	2.08226e-03
S34	1.21561e-02
S36	3.02859e-05
Cl35	1.71869e-01
Cl37	5.81312e-02
K39	1.85874e-01
K40	2.39181e-05
K41	1.41020e-02
Fe54	1.69367e-03
Fe56	2.75705e-02
Fe57	6.48111e-04
Fe58	8.77633e-05
<hr/>	
Thymus	
H1	1.04276e+01
H2	2.39678e-03
C12	2.21109e+01
C13	2.59141e-01
N14	2.81897e+00
N15	1.10318e-02
O16	6.31883e+01
O17	2.55812e-02
O18	1.46123e-01
Na23	1.00000e-01
P31	1.80000e-01

S32	2.65203e-01
S33	2.15938e-03
S34	1.26063e-02
S36	3.14076e-05
Cl35	1.64396e-01
Cl37	5.56038e-02
K39	1.85874e-01
K40	2.39181e-05
K41	1.41020e-02
Fe54	1.12911e-03
Fe56	1.83803e-02
Fe57	4.32074e-04
Fe58	5.85089e-05
<hr/>	
Lung	
H1	1.02376e+01
H2	2.35312e-03
C12	1.06650e+01
C13	1.24995e-01
N14	3.20745e+00
N15	1.25521e-02
O16	7.44676e+01
O17	3.01476e-02
O18	1.72206e-01
Na23	1.40000e-01
P31	1.40000e-01
S32	2.27317e-01
S33	1.85090e-03
S34	1.08054e-02
S36	2.69208e-05
Cl35	2.24177e-01
Cl37	7.58233e-02
K39	1.85874e-01
K40	2.39181e-05
K41	1.41020e-02
Fe54	3.38733e-03
Fe56	5.51409e-02
Fe57	1.29622e-03
Fe58	1.75527e-04
<hr/>	
Trachea	
H1	1.04876e+01
H2	2.41057e-03
C12	2.46709e+01

C13	2.89144e-01
N14	2.71936e+00
N15	1.06420e-02
O16	6.06652e+01
O17	2.45598e-02
O18	1.40288e-01
Na23	1.00000e-01
P31	2.00000e-01
S32	2.84146e-01
S33	2.31362e-03
S34	1.35067e-02
S36	3.36510e-05
Cl35	1.49451e-01
Cl37	5.05489e-02
K39	1.85874e-01
K40	2.39181e-05
K41	1.41020e-02

Breast_Fat_M

H1	1.13774e+01
H2	2.61509e-03
C12	5.81781e+01
C13	6.81852e-01
N14	7.47076e-01
N15	2.92362e-03
O16	2.86222e+01
O17	1.15875e-02
O18	6.61887e-02
Na23	1.00000e-01
P31	1.00000e-01
S32	9.47153e-02
S33	7.71207e-04
S34	4.50224e-03
S36	1.12170e-05
Cl35	7.47256e-03
Cl37	2.52744e-03

Breast_Glandular_M

H1	1.05976e+01
H2	2.43585e-03
C12	3.28154e+01
C13	3.84599e-01
N14	2.98831e+00
N15	1.16945e-02

O16	5.25572e+01
O17	2.12773e-02
O18	1.21538e-01
Na23	1.00000e-01
P31	1.00000e-01
S32	1.89431e-01
S33	1.54241e-03
S34	9.00448e-03
S36	2.24340e-05
Cl35	7.47256e-02
Cl37	2.52744e-02

Heart	
H1	1.03676e+01
H2	2.38299e-03
C12	1.32547e+01
C13	1.55345e-01
N14	2.95842e+00
N15	1.15775e-02
O16	7.20642e+01
O17	2.91746e-02
O18	1.66648e-01
Na23	1.00000e-01
P31	1.80000e-01
S32	1.89431e-01
S33	1.54241e-03
S34	9.00448e-03
S36	2.24340e-05
Cl35	1.64396e-01
Cl37	5.56038e-02
K39	2.60224e-01
K40	3.34854e-05
K41	1.97427e-02
Fe54	1.12911e-03
Fe56	1.83803e-02
Fe57	4.32074e-04
Fe58	5.85089e-05

Liver	
H1	1.02676e+01
H2	2.36001e-03
C12	1.60519e+01
C13	1.88129e-01
N14	2.94846e+00

N15	1.15386e-02
O16	6.92119e+01
O17	2.80199e-02
O18	1.60052e-01
Na23	1.70000e-01
P31	1.70000e-01
S32	2.55731e-01
S33	2.08226e-03
S34	1.21561e-02
S36	3.02859e-05
Cl35	1.71869e-01
Cl37	5.81312e-02
K39	2.50930e-01
K40	3.22895e-05
K41	1.90376e-02
Fe54	1.69367e-03
Fe56	2.75705e-02
Fe57	6.48111e-04
Fe58	8.77633e-05
<hr/>	
Stomach	
H1	1.04776e+01
H2	2.40827e-03
C12	1.12185e+01
C13	1.31482e-01
N14	2.51018e+00
N15	9.82337e-03
O16	7.47170e+01
O17	3.02485e-02
O18	1.72783e-01
Na23	1.00000e-01
P31	1.00000e-01
S32	1.23130e-01
S33	1.00257e-03
S34	5.85291e-03
S36	1.45821e-05
Cl35	1.71869e-01
Cl37	5.81312e-02
K39	1.20818e-01
K40	1.55468e-05
K41	9.16627e-03
Fe54	1.69367e-03
Fe56	2.75705e-02

	Fe57	6.48111e-04
	Fe58	8.77633e-05
Spleen		
	H1	1.02476e+01
	H2	2.35542e-03
	C12	1.10110e+01
	C13	1.29049e-01
	N14	3.23733e+00
	N15	1.26690e-02
	O16	7.41086e+01
	O17	3.00022e-02
	O18	1.71376e-01
	Na23	1.00000e-01
	P31	2.00000e-01
	S32	1.89431e-01
	S33	1.54241e-03
	S34	9.00448e-03
	S36	2.24340e-05
	Cl35	1.86814e-01
	Cl37	6.31861e-02
	K39	2.32343e-01
	K40	2.98976e-05
	K41	1.76274e-02
	Fe54	2.82278e-03
	Fe56	4.59508e-02
	Fe57	1.08018e-03
	Fe58	1.46272e-04
Gall_Bladder_Wall		
	H1	1.04276e+01
	H2	2.39678e-03
	C12	2.21109e+01
	C13	2.59141e-01
	N14	2.81897e+00
	N15	1.10318e-02
	O16	6.31883e+01
	O17	2.55812e-02
	O18	1.46123e-01
	Na23	1.00000e-01
	P31	1.80000e-01
	S32	2.65203e-01
	S33	2.15938e-03
	S34	1.26063e-02

S36	3.14076e-05
Cl35	1.64396e-01
Cl37	5.56038e-02
K39	1.85874e-01
K40	2.39181e-05
K41	1.41020e-02
Fe54	1.12911e-03
Fe56	1.83803e-02
Fe57	4.32074e-04
Fe58	5.85089e-05
<hr/>	
Adrenals	
H1	1.04276e+01
H2	2.39678e-03
C12	2.18341e+01
C13	2.55897e-01
N14	2.82893e+00
N15	1.10708e-02
O16	6.34576e+01
O17	2.56903e-02
O18	1.46745e-01
Na23	1.00000e-01
P31	1.80000e-01
S32	2.65203e-01
S33	2.15938e-03
S34	1.26063e-02
S36	3.14076e-05
Cl35	1.64396e-01
Cl37	5.56038e-02
K39	1.85874e-01
K40	2.39181e-05
K41	1.41020e-02
Fe54	1.12911e-03
Fe56	1.83803e-02
Fe57	4.32074e-04
Fe58	5.85089e-05
<hr/>	
Kidney	
H1	1.02576e+01
H2	2.35772e-03
C12	1.22564e+01
C13	1.43645e-01
N14	3.09788e+00
N15	1.21233e-02

O16	7.29617e+01
O17	2.95379e-02
O18	1.68724e-01
Na23	1.60000e-01
P31	1.60000e-01
S32	1.89431e-01
S33	1.54241e-03
S34	9.00448e-03
S36	2.24340e-05
Cl35	1.79341e-01
Cl37	6.06587e-02
K39	1.85874e-01
K40	2.39181e-05
K41	1.41020e-02
Ca40	5.79971e-02
Ca42	4.06416e-04
Ca43	8.68221e-05
Ca44	1.37269e-03
Ca46	2.75185e-06
Ca48	1.34245e-04
Fe54	2.25822e-03
Fe56	3.67606e-02
Fe57	8.64147e-04
Fe58	1.17018e-04
<hr/>	
Small_Intestine	
H1	1.04676e+01
H2	2.40597e-03
C12	1.12086e+01
C13	1.31366e-01
N14	2.55002e+00
N15	9.97929e-03
O16	7.46970e+01
O17	3.02405e-02
O18	1.72736e-01
Na23	1.00000e-01
P31	1.00000e-01
S32	1.23130e-01
S33	1.00257e-03
S34	5.85291e-03
S36	1.45821e-05
Cl35	1.71869e-01
Cl37	5.81312e-02

K39	1.20818e-01
K40	1.55468e-05
K41	9.16627e-03
Fe54	1.69367e-03
Fe56	2.75705e-02
Fe57	6.48111e-04
Fe58	8.77633e-05
<hr/>	
Pancreas	
H1	1.04976e+01
H2	2.41287e-03
C12	1.53106e+01
C13	1.79441e-01
N14	2.45041e+00
N15	9.58948e-03
O16	7.04286e+01
O17	2.85124e-02
O18	1.62866e-01
Na23	1.80000e-01
P31	1.80000e-01
S32	1.13658e-01
S33	9.25449e-04
S34	5.40269e-03
S36	1.34604e-05
Cl35	1.64396e-01
Cl37	5.56038e-02
K39	1.85874e-01
K40	2.39181e-05
K41	1.41020e-02
Fe54	1.12911e-03
Fe56	1.83803e-02
Fe57	4.32074e-04
Fe58	5.85089e-05
<hr/>	
Large_Intestine	
H1	1.04676e+01
H2	2.40597e-03
C12	1.11987e+01
C13	1.31250e-01
N14	2.55998e+00
N15	1.00183e-02
O16	7.46970e+01
O17	3.02405e-02
O18	1.72736e-01

Na23	1.00000e-01
P31	1.00000e-01
S32	1.23130e-01
S33	1.00257e-03
S34	5.85291e-03
S36	1.45821e-05
Cl35	1.71869e-01
Cl37	5.81312e-02
K39	1.20818e-01
K40	1.55468e-05
K41	9.16627e-03
Fe54	1.69367e-03
Fe56	2.75705e-02
Fe57	6.48111e-04
Fe58	8.77633e-05
<hr/>	
Urinary	
H1	1.04876e+01
H2	2.41057e-03
C12	9.51844e+00
C13	1.11557e-01
N14	2.60979e+00
N15	1.02132e-02
O16	7.58539e+01
O17	3.07088e-02
O18	1.75412e-01
Na23	2.00000e-01
P31	2.00000e-01
S32	1.89431e-01
S33	1.54241e-03
S34	9.00448e-03
S36	2.24340e-05
Cl35	2.24177e-01
Cl37	7.58233e-02
K39	2.78811e-01
K40	3.58772e-05
K41	2.11529e-02
<hr/>	
Uterus	
H1	1.05576e+01
H2	2.42666e-03
C12	2.92275e+01
C13	3.42548e-01
N14	2.47033e+00

N15	9.66744e-03
O16	5.64067e+01
O17	2.28358e-02
O18	1.30440e-01
Na23	1.00000e-01
P31	1.90000e-01
S32	1.89431e-01
S33	1.54241e-03
S34	9.00448e-03
S36	2.24340e-05
Cl35	8.96707e-02
Cl37	3.03293e-02
K39	1.85874e-01
K40	2.39181e-05
K41	1.41020e-02
Fe54	5.64556e-04
Fe56	9.19015e-03
Fe57	2.16037e-04
Fe58	2.92544e-05
<hr/>	
Ovaries	
H1	1.04776e+01
H2	2.40827e-03
C12	2.42261e+01
C13	2.83931e-01
N14	2.72932e+00
N15	1.06810e-02
O16	6.11040e+01
O17	2.47374e-02
O18	1.41303e-01
Na23	1.00000e-01
P31	1.90000e-01
S32	2.74674e-01
S33	2.23650e-03
S34	1.30565e-02
S36	3.25293e-05
Cl35	1.56924e-01
Cl37	5.30763e-02
K39	1.85874e-01
K40	2.39181e-05
K41	1.41020e-02
Fe54	5.64556e-04
Fe56	9.19015e-03

	Fe57	2.16037e-04
	Fe58	2.92544e-05
Ureters		
	H1	1.04976e+01
	H2	2.41287e-03
	C12	2.53034e+01
	C13	2.96558e-01
	N14	2.68947e+00
	N15	1.05250e-02
	O16	6.00369e+01
	O17	2.43054e-02
	O18	1.38835e-01
	Na23	1.00000e-01
	P31	2.00000e-01
	S32	2.84146e-01
	S33	2.31362e-03
	S34	1.35067e-02
	S36	3.36510e-05
	Cl35	1.49451e-01
	Cl37	5.05489e-02
	K39	1.85874e-01
	K40	2.39181e-05
	K41	1.41020e-02
Urethra		
	H1	1.04976e+01
	H2	2.41287e-03
	C12	2.53034e+01
	C13	2.96558e-01
	N14	2.68947e+00
	N15	1.05250e-02
	O16	6.00369e+01
	O17	2.43054e-02
	O18	1.38835e-01
	Na23	1.00000e-01
	P31	2.00000e-01
	S32	2.84146e-01
	S33	2.31362e-03
	S34	1.35067e-02
	S36	3.36510e-05
	Cl35	1.49451e-01
	Cl37	5.05489e-02
	K39	1.85874e-01

K40	2.39181e-05
K41	1.41020e-02
Epididymes	
H1	1.04976e+01
H2	2.41287e-03
C12	2.53034e+01
C13	2.96558e-01
N14	2.68947e+00
N15	1.05250e-02
O16	6.00369e+01
O17	2.43054e-02
O18	1.38835e-01
Na23	1.00000e-01
P31	2.00000e-01
S32	2.84146e-01
S33	2.31362e-03
S34	1.35067e-02
S36	3.36510e-05
Cl35	1.49451e-01
Cl37	5.05489e-02
K39	1.85874e-01
K40	2.39181e-05
K41	1.41020e-02
Fallopian_tubes	
H1	1.05976e+01
H2	2.43585e-03
C12	3.11351e+01
C13	3.64905e-01
N14	2.39064e+00
N15	9.35559e-03
O16	5.45518e+01
O17	2.20848e-02
O18	1.26151e-01
Na23	1.00000e-01
P31	2.00000e-01
S32	1.89431e-01
S33	1.54241e-03
S34	9.00448e-03
S36	2.24340e-05
Cl35	7.47256e-02
Cl37	2.52744e-02
K39	1.85874e-01

K40	2.39181e-05
K41	1.41020e-02
Prostate	
H1	1.04276e+01
H2	2.39678e-03
C12	2.21109e+01
C13	2.59141e-01
N14	2.81897e+00
N15	1.10318e-02
O16	6.31883e+01
O17	2.55812e-02
O18	1.46123e-01
Na23	1.00000e-01
P31	1.80000e-01
S32	2.65203e-01
S33	2.15938e-03
S34	1.26063e-02
S36	3.14076e-05
Cl35	1.64396e-01
Cl37	5.56038e-02
K39	1.85874e-01
K40	2.39181e-05
K41	1.41020e-02
Fe54	1.12911e-03
Fe56	1.83803e-02
Fe57	4.32074e-04
Fe58	5.85089e-05
Penis	
H1	1.01977e+01
H2	2.34393e-03
C12	1.34128e+01
C13	1.57199e-01
N14	3.36682e+00
N15	1.31758e-02
O16	7.15755e+01
O17	2.89767e-02
O18	1.65518e-01
Na23	1.00000e-01
P31	1.80000e-01
S32	2.65203e-01
S33	2.15938e-03
S34	1.26063e-02

S36	3.14076e-05
Cl35	1.04616e-01
Cl37	3.53842e-02
K39	3.34573e-01
K40	4.30526e-05
K41	2.53835e-02
Fe54	1.12911e-03
Fe56	1.83803e-02
Fe57	4.32074e-04
Fe58	5.85089e-05
<hr/>	
Scrotum	
H1	1.04276e+01
H2	2.39678e-03
C12	2.21109e+01
C13	2.59141e-01
N14	2.81897e+00
N15	1.10318e-02
O16	6.31883e+01
O17	2.55812e-02
O18	1.46123e-01
Na23	1.00000e-01
P31	1.80000e-01
S32	2.65203e-01
S33	2.15938e-03
S34	1.26063e-02
S36	3.14076e-05
Cl35	1.64396e-01
Cl37	5.56038e-02
K39	1.85874e-01
K40	2.39181e-05
K41	1.41020e-02
Fe54	1.12911e-03
Fe56	1.83803e-02
Fe57	4.32074e-04
Fe58	5.85089e-05
<hr/>	
Testes	
H1	1.05676e+01
H2	2.42895e-03
C12	9.85450e+00
C13	1.15495e-01
N14	2.07189e+00
N15	8.10818e-03

O16	7.62628e+01
O17	3.08743e-02
O18	1.76357e-01
Na23	1.90000e-01
P31	1.00000e-01
S32	1.89431e-01
S33	1.54241e-03
S34	9.00448e-03
S36	2.24340e-05
Cl35	1.56924e-01
Cl37	5.30763e-02
K39	1.85874e-01
K40	2.39181e-05
K41	1.41020e-02
Fe54	5.64556e-04
Fe56	9.19015e-03
Fe57	2.16037e-04
Fe58	2.92544e-05

Cartilage

H1	9.60779e+00
H2	2.20835e-03
C12	9.80508e+00
C13	1.14916e-01
N14	2.21135e+00
N15	8.65392e-03
O16	7.41984e+01
O17	3.00386e-02
O18	1.71583e-01
Na23	4.90000e-01
P31	2.16000e+00
S32	8.42966e-01
S33	6.86374e-03
S34	4.00700e-02
S36	9.98313e-05
Cl35	2.24177e-01
Cl37	7.58233e-02

Cortical_bone

H1	3.56918e+00
H2	8.20375e-04
C12	1.57652e+01
C13	1.84769e-01
N14	4.17367e+00

N15	1.63333e-02
O16	4.46886e+01
O17	1.80918e-02
O18	1.03342e-01
Na23	3.00000e-01
Mg24	1.55900e-01
Mg25	2.05602e-02
Mg26	2.35398e-02
P31	9.40000e+00
S32	2.84146e-01
S33	2.31362e-03
S34	1.35067e-02
S36	3.36510e-05
Ca40	2.05696e+01
Ca42	1.44142e-01
Ca43	3.07929e-02
Ca44	4.86847e-01
Ca46	9.75991e-04
Ca48	4.76122e-02
<hr/>	
Teeth	
H1	2.19949e+00
H2	5.05553e-04
C12	9.38995e+00
C13	1.10051e-01
N14	2.88870e+00
N15	1.13047e-02
O16	4.19859e+01
O17	1.69976e-02
O18	9.70922e-02
Mg24	5.45650e-01
Mg25	7.19607e-02
Mg26	8.23894e-02
P31	1.37000e+01
K39	2.68588e+01
K40	3.45617e-03
K41	2.03773e+00
<hr/>	
spmc_Cranium	
H1	5.93864e+00
H2	1.36499e-03
C12	2.64895e+01
C13	3.10459e-01
N14	3.45647e+00

N15	1.35266e-02
O16	4.20657e+01
O17	1.70299e-02
O18	9.72767e-02
Na23	2.30000e-01
Mg24	1.24720e-01
Mg25	1.64482e-02
Mg26	1.88319e-02
P31	6.44000e+00
S32	2.36788e-01
S33	1.92802e-03
S34	1.12556e-02
S36	2.80425e-05
Cl35	7.47256e-03
Cl37	2.52744e-03
K39	9.29371e-03
K40	1.19591e-06
K41	7.05098e-04
Ca40	1.39966e+01
Ca42	9.80816e-02
Ca43	2.09531e-02
Ca44	3.31276e-01
Ca46	6.64114e-04
Ca48	3.23978e-02
Fe54	1.12911e-03
Fe56	1.83803e-02
Fe57	4.32074e-04
Fe58	5.85089e-05
<hr/>	
spmc_Mandible	
H1	9.95771e+00
H2	2.28878e-03
C12	4.55165e+01
C13	5.33457e-01
N14	2.22131e+00
N15	8.69290e-03
O16	3.67102e+01
O17	1.48618e-02
O18	8.48923e-02
Na23	1.30000e-01
Mg24	7.01550e-02
Mg25	9.25209e-03
Mg26	1.05929e-02

P31	1.46000e+00
S32	1.61016e-01
S33	1.31105e-03
S34	7.65381e-03
S36	1.90689e-05
Cl35	2.24177e-02
Cl37	7.58233e-03
K39	1.85874e-02
K40	2.39181e-06
K41	1.41020e-03
Ca40	2.92885e+00
Ca42	2.05240e-02
Ca43	4.38452e-03
Ca44	6.93208e-02
Ca46	1.38969e-04
Ca48	6.77937e-03
Fe54	2.25822e-03
Fe56	3.67606e-02
Fe57	8.64147e-04
Fe58	1.17018e-04
<hr/>	
spmc_Vertebrae_C	
H1	8.85796e+00
H2	2.03600e-03
C12	3.55731e+01
C13	4.16919e-01
N14	3.07795e+00
N15	1.20453e-02
O16	4.32624e+01
O17	1.75144e-02
O18	1.00044e-01
Na23	1.50000e-01
Mg24	1.09130e-01
Mg25	1.43921e-02
Mg26	1.64779e-02
P31	2.56000e+00
S32	1.98902e-01
S33	1.61954e-03
S34	9.45471e-03
S36	2.35557e-05
Cl35	2.24177e-02
Cl37	7.58233e-03
K39	1.85874e-02

K40	2.39181e-06
K41	1.41020e-03
Ca40	5.33573e+00
Ca42	3.73902e-02
Ca43	7.98764e-03
Ca44	1.26287e-01
Ca46	2.53171e-04
Ca48	1.23505e-02
Fe54	3.38733e-03
Fe56	5.51409e-02
Fe57	1.29622e-03
Fe58	1.75527e-04
<hr/>	
spmc_Vertebrae_T	
H1	9.67778e+00
H2	2.22443e-03
C12	3.86767e+01
C13	4.53293e-01
N14	2.90862e+00
N15	1.13826e-02
O16	4.30231e+01
O17	1.74175e-02
O18	9.94907e-02
Na23	1.30000e-01
Mg24	1.01335e-01
Mg25	1.33641e-02
Mg26	1.53009e-02
P31	1.49000e+00
S32	1.79959e-01
S33	1.46529e-03
S34	8.55426e-03
S36	2.13123e-05
Cl35	2.98902e-02
Cl37	1.01098e-02
K39	1.85874e-02
K40	2.39181e-06
K41	1.41020e-03
Ca40	2.95785e+00
Ca42	2.07272e-02
Ca43	4.42793e-03
Ca44	7.00072e-02
Ca46	1.40345e-04
Ca48	6.84649e-03

Fe54	3.38733e-03
Fe56	5.51409e-02
Fe57	1.29622e-03
Fe58	1.75527e-04
<hr/>	
spmc_Vertebrae_L	
H1	9.59779e+00
H2	2.20605e-03
C12	3.77871e+01
C13	4.42868e-01
N14	2.93850e+00
N15	1.14996e-02
O16	4.36514e+01
O17	1.76719e-02
O18	1.00944e-01
Na23	1.30000e-01
Mg24	1.01335e-01
Mg25	1.33641e-02
Mg26	1.53009e-02
P31	1.59000e+00
S32	1.79959e-01
S33	1.46529e-03
S34	8.55426e-03
S36	2.13123e-05
Cl35	2.98902e-02
Cl37	1.01098e-02
K39	2.78811e-02
K40	3.58772e-06
K41	2.11529e-03
Ca40	3.18017e+00
Ca42	2.22851e-02
Ca43	4.76075e-03
Ca44	7.52691e-02
Ca46	1.50893e-04
Ca48	7.36110e-03
Fe54	3.38733e-03
Fe56	5.51409e-02
Fe57	1.29622e-03
Fe58	1.75527e-04
<hr/>	
spmc_Sternum	
H1	9.81774e+00
H2	2.25661e-03
C12	3.89436e+01

C13	4.56421e-01
N14	2.88870e+00
N15	1.13047e-02
O16	4.32325e+01
O17	1.75023e-02
O18	9.99750e-02
Na23	1.20000e-01
Mg24	1.01335e-01
Mg25	1.33641e-02
Mg26	1.53009e-02
P31	1.31000e+00
S32	1.79959e-01
S33	1.46529e-03
S34	8.55426e-03
S36	2.13123e-05
Cl35	2.98902e-02
Cl37	1.01098e-02
K39	2.78811e-02
K40	3.58772e-06
K41	2.11529e-03
Ca40	2.56154e+00
Ca42	1.79500e-02
Ca43	3.83464e-03
Ca44	6.06271e-02
Ca46	1.21540e-04
Ca48	5.92915e-03
Fe54	3.95189e-03
Fe56	6.43311e-02
Fe57	1.51226e-03
Fe58	2.04781e-04

spmc_Ribs

H1	9.47782e+00
H2	2.17848e-03
C12	3.74610e+01
C13	4.39045e-01
N14	2.95842e+00
N15	1.15775e-02
O16	4.35716e+01
O17	1.76396e-02
O18	1.00759e-01
Na23	1.30000e-01
Mg24	1.01335e-01

Mg25	1.33641e-02
Mg26	1.53009e-02
P31	1.74000e+00
S32	1.89431e-01
S33	1.54241e-03
S34	9.00448e-03
S36	2.24340e-05
Cl35	2.98902e-02
Cl37	1.01098e-02
K39	2.78811e-02
K40	3.58772e-06
K41	2.11529e-03
Ca40	3.50882e+00
Ca42	2.45881e-02
Ca43	5.25274e-03
Ca44	8.30477e-02
Ca46	1.66487e-04
Ca48	8.12182e-03
Fe54	3.38733e-03
Fe56	5.51409e-02
Fe57	1.29622e-03
Fe58	1.75527e-04
<hr/>	
spmc_Scapulae	
H1	9.26787e+00
H2	2.13022e-03
C12	4.20373e+01
C13	4.92680e-01
N14	2.44045e+00
N15	9.55050e-03
O16	3.78571e+01
O17	1.53261e-02
O18	8.75444e-02
Na23	1.50000e-01
Mg24	7.79500e-02
Mg25	1.02801e-02
Mg26	1.17699e-02
P31	2.30000e+00
S32	1.70488e-01
S33	1.38817e-03
S34	8.10404e-03
S36	2.01906e-05
Cl35	2.24177e-02

Cl37	7.58233e-03
K39	1.85874e-02
K40	2.39181e-06
K41	1.41020e-03
Ca40	4.81376e+00
Ca42	3.37325e-02
Ca43	7.20624e-03
Ca44	1.13933e-01
Ca46	2.28404e-04
Ca48	1.11423e-02
Fe54	2.25822e-03
Fe56	3.67606e-02
Fe57	8.64147e-04
Fe58	1.17018e-04
<hr/>	
spmc_Clavicles	
H1	9.68777e+00
H2	2.22673e-03
C12	4.55165e+01
C13	5.33457e-01
N14	2.20139e+00
N15	8.61494e-03
O16	3.56930e+01
O17	1.44500e-02
O18	8.25399e-02
Na23	1.40000e-01
Mg24	7.01550e-02
Mg25	9.25209e-03
Mg26	1.05929e-02
P31	1.85000e+00
S32	1.61016e-01
S33	1.31105e-03
S34	7.65381e-03
S36	1.90689e-05
Cl35	1.49451e-02
Cl37	5.05489e-03
K39	9.29371e-03
K40	1.19591e-06
K41	7.05098e-04
Ca40	3.81814e+00
Ca42	2.67557e-02
Ca43	5.71579e-03
Ca44	9.03687e-02

Ca46	1.81164e-04
Ca48	8.83779e-03
Fe54	1.69367e-03
Fe56	2.75705e-02
Fe57	6.48111e-04
Fe58	8.77633e-05
<hr/>	
spmc_Os_Coxae	
H1	9.76775e+00
H2	2.24512e-03
C12	4.27885e+01
C13	5.01484e-01
N14	2.48029e+00
N15	9.70642e-03
O16	3.89342e+01
O17	1.57622e-02
O18	9.00351e-02
Na23	1.30000e-01
Mg24	7.79500e-02
Mg25	1.02801e-02
Mg26	1.17699e-02
P31	1.59000e+00
S32	1.70488e-01
S33	1.38817e-03
S34	8.10404e-03
S36	2.01906e-05
Cl35	2.24177e-02
Cl37	7.58233e-03
K39	1.85874e-02
K40	2.39181e-06
K41	1.41020e-03
Ca40	3.20917e+00
Ca42	2.24883e-02
Ca43	4.80416e-03
Ca44	7.59555e-02
Ca46	1.52269e-04
Ca48	7.42822e-03
Fe54	2.82278e-03
Fe56	4.59508e-02
Fe57	1.08018e-03
Fe58	1.46272e-04
<hr/>	
spmc_Sacrum	
H1	9.45783e+00

H2	2.17388e-03
C12	3.71743e+01
C13	4.35685e-01
N14	2.96838e+00
N15	1.16165e-02
O16	4.37910e+01
O17	1.77284e-02
O18	1.01266e-01
Na23	1.30000e-01
Mg24	1.01335e-01
Mg25	1.33641e-02
Mg26	1.53009e-02
P31	1.76000e+00
S32	1.89431e-01
S33	1.54241e-03
S34	9.00448e-03
S36	2.24340e-05
Cl35	2.98902e-02
Cl37	1.01098e-02
K39	2.78811e-02
K40	3.58772e-06
K41	2.11529e-03
Ca40	3.55715e+00
Ca42	2.49268e-02
Ca43	5.32509e-03
Ca44	8.41916e-02
Ca46	1.68780e-04
Ca48	8.23369e-03
Fe54	3.38733e-03
Fe56	5.51409e-02
Fe57	1.29622e-03
Fe58	1.75527e-04
<hr/>	
spmc_Humera_proximal	
H1	9.96771e+00
H2	2.29108e-03
C12	4.82248e+01
C13	5.65198e-01
N14	1.95236e+00
N15	7.64040e-03
O16	3.38181e+01
O17	1.36910e-02
O18	7.82042e-02

Na23	1.30000e-01
Mg24	5.45650e-02
Mg25	7.19607e-03
Mg26	8.23894e-03
P31	1.59000e+00
S32	1.51545e-01
S33	1.23393e-03
S34	7.20359e-03
S36	1.79472e-05
Cl35	1.49451e-02
Cl37	5.05489e-03
K39	9.29371e-03
K40	1.19591e-06
K41	7.05098e-04
Ca40	3.24784e+00
Ca42	2.27593e-02
Ca43	4.86204e-03
Ca44	7.68706e-02
Ca46	1.54104e-04
Ca48	7.51772e-03
Fe54	1.69367e-03
Fe56	2.75705e-02
Fe57	6.48111e-04
Fe58	8.77633e-05
<hr/>	
spmc_Humera_distal	
H1	9.48782e+00
H2	2.18077e-03
C12	5.02313e+01
C13	5.88714e-01
N14	1.63361e+00
N15	6.39299e-03
O16	2.98988e+01
O17	1.21043e-02
O18	6.91407e-02
Na23	1.50000e-01
Mg24	3.89750e-02
Mg25	5.14005e-03
Mg26	5.88496e-03
P31	2.41000e+00
S32	1.42073e-01
S33	1.15681e-03
S34	6.75336e-03

S36	1.68255e-05
Cl35	7.47256e-03
Cl37	2.52744e-03
K39	9.29371e-03
K40	1.19591e-06
K41	7.05098e-04
Ca40	5.11341e+00
Ca42	3.58323e-02
Ca43	7.65482e-03
Ca44	1.21025e-01
Ca46	2.42622e-04
Ca48	1.18359e-02
<hr/>	
spmc_Radii_proximal	
H1	1.02476e+01
H2	2.35542e-03
C12	5.49263e+01
C13	6.43739e-01
N14	1.29493e+00
N15	5.06761e-03
O16	2.76848e+01
O17	1.12079e-02
O18	6.40209e-02
Na23	1.30000e-01
Mg24	2.33850e-02
Mg25	3.08403e-03
Mg26	3.53097e-03
P31	1.53000e+00
S32	1.23130e-01
S33	1.00257e-03
S34	5.85291e-03
S36	1.45821e-05
Cl35	7.47256e-03
Cl37	2.52744e-03
K39	9.29371e-03
K40	1.19591e-06
K41	7.05098e-04
Ca40	3.16084e+00
Ca42	2.21497e-02
Ca43	4.73181e-03
Ca44	7.48116e-02
Ca46	1.49976e-04
Ca48	7.31635e-03

spmc_Radii_distal	
H1	9.90772e+00
H2	2.27729e-03
C12	5.28209e+01
C13	6.19065e-01
N14	1.45431e+00
N15	5.69132e-03
O16	2.86821e+01
O17	1.16117e-02
O18	6.63271e-02
Na23	1.40000e-01
Mg24	3.11800e-02
Mg25	4.11204e-03
Mg26	4.70797e-03
P31	1.93000e+00
S32	1.32601e-01
S33	1.07969e-03
S34	6.30314e-03
S36	1.57038e-05
Cl35	7.47256e-03
Cl37	2.52744e-03
K39	9.29371e-03
K40	1.19591e-06
K41	7.05098e-04
Ca40	4.04046e+00
Ca42	2.83136e-02
Ca43	6.04861e-03
Ca44	9.56307e-02
Ca46	1.91712e-04
Ca48	9.35240e-03
spmc_Ulnae_proximal	
H1	9.37784e+00
H2	2.15550e-03
C12	4.95295e+01
C13	5.80489e-01
N14	1.68341e+00
N15	6.58789e-03
O16	3.02378e+01
O17	1.22415e-02
O18	6.99248e-02
Na23	1.50000e-01
Mg24	3.89750e-02

Mg25	5.14005e-03
Mg26	5.88496e-03
P31	2.54000e+00
S32	1.51545e-01
S33	1.23393e-03
S34	7.20359e-03
S36	1.79472e-05
Cl35	7.47256e-03
Cl37	2.52744e-03
K39	9.29371e-03
K40	1.19591e-06
K41	7.05098e-04
Ca40	5.39373e+00
Ca42	3.77967e-02
Ca43	8.07446e-03
Ca44	1.27660e-01
Ca46	2.55922e-04
Ca48	1.24848e-02
<hr/>	
spmc_Ulnae_distal	
H1	9.62779e+00
H2	2.21294e-03
C12	5.11307e+01
C13	5.99256e-01
N14	1.57384e+00
N15	6.15910e-03
O16	2.94599e+01
O17	1.19266e-02
O18	6.81260e-02
Na23	1.50000e-01
Mg24	3.89750e-02
Mg25	5.14005e-03
Mg26	5.88496e-03
P31	2.25000e+00
S32	1.42073e-01
S33	1.15681e-03
S34	6.75336e-03
S36	1.68255e-05
Cl35	7.47256e-03
Cl37	2.52744e-03
K39	9.29371e-03
K40	1.19591e-06
K41	7.05098e-04

Ca40	4.74609e+00
Ca42	3.32583e-02
Ca43	7.10495e-03
Ca44	1.12332e-01
Ca46	2.25193e-04
Ca48	1.09857e-02
<hr/>	
spmc_Wrists_and_hands	
H1	9.48782e+00
H2	2.18077e-03
C12	5.02708e+01
C13	5.89177e-01
N14	1.63361e+00
N15	6.39299e-03
O16	2.98489e+01
O17	1.20841e-02
O18	6.90254e-02
Na23	1.50000e-01
Mg24	3.89750e-02
Mg25	5.14005e-03
Mg26	5.88496e-03
P31	2.41000e+00
S32	1.42073e-01
S33	1.15681e-03
S34	6.75336e-03
S36	1.68255e-05
Cl35	7.47256e-03
Cl37	2.52744e-03
K39	9.29371e-03
K40	1.19591e-06
K41	7.05098e-04
Ca40	5.11341e+00
Ca42	3.58323e-02
Ca43	7.65482e-03
Ca44	1.21025e-01
Ca46	2.42622e-04
Ca48	1.18359e-02
<hr/>	
spmc_Femora_proximal	
H1	9.36785e+00
H2	2.15320e-03
C12	4.49927e+01
C13	5.27317e-01
N14	2.16154e+00

N15	8.45901e-03
O16	3.50547e+01
O17	1.41916e-02
O18	8.10639e-02
Na23	1.50000e-01
Mg24	6.23600e-02
Mg25	8.22408e-03
Mg26	9.41593e-03
P31	2.31000e+00
S32	1.61016e-01
S33	1.31105e-03
S34	7.65381e-03
S36	1.90689e-05
Cl35	1.49451e-02
Cl37	5.05489e-03
K39	9.29371e-03
K40	1.19591e-06
K41	7.05098e-04
Ca40	4.85242e+00
Ca42	3.40034e-02
Ca43	7.26412e-03
Ca44	1.14848e-01
Ca46	2.30238e-04
Ca48	1.12318e-02
Fe54	1.12911e-03
Fe56	1.83803e-02
Fe57	4.32074e-04
Fe58	5.85089e-05
<hr/>	
spmc_Femora_distal	
H1	9.54781e+00
H2	2.19456e-03
C12	5.05871e+01
C13	5.92884e-01
N14	1.61368e+00
N15	6.31502e-03
O16	2.97392e+01
O17	1.20397e-02
O18	6.87717e-02
Na23	1.50000e-01
Mg24	3.89750e-02
Mg25	5.14005e-03
Mg26	5.88496e-03

P31	2.34000e+00
S32	1.42073e-01
S33	1.15681e-03
S34	6.75336e-03
S36	1.68255e-05
Cl35	7.47256e-03
Cl37	2.52744e-03
K39	9.29371e-03
K40	1.19591e-06
K41	7.05098e-04
Ca40	4.95875e+00
Ca42	3.47485e-02
Ca43	7.42329e-03
Ca44	1.17365e-01
Ca46	2.35283e-04
Ca48	1.14779e-02
<hr/>	
spmc_Patellae	
H1	9.54781e+00
H2	2.19456e-03
C12	5.05871e+01
C13	5.92884e-01
N14	1.61368e+00
N15	6.31502e-03
O16	2.97292e+01
O17	1.20356e-02
O18	6.87487e-02
Na23	1.50000e-01
Mg24	3.89750e-02
Mg25	5.14005e-03
Mg26	5.88496e-03
P31	2.34000e+00
S32	1.42073e-01
S33	1.15681e-03
S34	6.75336e-03
S36	1.68255e-05
Cl35	7.47256e-03
Cl37	2.52744e-03
K39	9.29371e-03
K40	1.19591e-06
K41	7.05098e-04
Ca40	4.95875e+00
Ca42	3.47485e-02

Ca43	7.42329e-03
Ca44	1.17365e-01
Ca46	2.35283e-04
Ca48	1.14779e-02
<hr/>	
spmc_Tibiae_proximal	
H1	9.90772e+00
H2	2.27729e-03
C12	5.28407e+01
C13	6.19296e-01
N14	1.44435e+00
N15	5.65233e-03
O16	2.86721e+01
O17	1.16077e-02
O18	6.63041e-02
Na23	1.40000e-01
Mg24	3.11800e-02
Mg25	4.11204e-03
Mg26	4.70797e-03
P31	1.92000e+00
S32	1.32601e-01
S33	1.07969e-03
S34	6.30314e-03
S36	1.57038e-05
Cl35	7.47256e-03
Cl37	2.52744e-03
K39	9.29371e-03
K40	1.19591e-06
K41	7.05098e-04
Ca40	4.02113e+00
Ca42	2.81782e-02
Ca43	6.01967e-03
Ca44	9.51731e-02
Ca46	1.90795e-04
Ca48	9.30765e-03
<hr/>	
spmc_Tibiae_distal	
H1	9.79775e+00
H2	2.25201e-03
C12	5.21389e+01
C13	6.11072e-01
N14	1.50411e+00
N15	5.88622e-03
O16	2.90012e+01

O17	1.17409e-02
O18	6.70651e-02
Na23	1.40000e-01
Mg24	3.11800e-02
Mg25	4.11204e-03
Mg26	4.70797e-03
P31	2.05000e+00
S32	1.32601e-01
S33	1.07969e-03
S34	6.30314e-03
S36	1.57038e-05
Cl35	7.47256e-03
Cl37	2.52744e-03
K39	9.29371e-03
K40	1.19591e-06
K41	7.05098e-04
Ca40	4.32078e+00
Ca42	3.02780e-02
Ca43	6.46825e-03
Ca44	1.02265e-01
Ca46	2.05013e-04
Ca48	1.00013e-02
<hr/>	
spmc_Fibulae_proximal	
H1	1.03776e+01
H2	2.38529e-03
C12	5.57565e+01
C13	6.53470e-01
N14	1.23517e+00
N15	4.83372e-03
O16	2.73058e+01
O17	1.10545e-02
O18	6.31445e-02
Na23	1.30000e-01
Mg24	2.33850e-02
Mg25	3.08403e-03
Mg26	3.53097e-03
P31	1.37000e+00
S32	1.23130e-01
S33	1.00257e-03
S34	5.85291e-03
S36	1.45821e-05
Cl35	7.47256e-03

Cl37	2.52744e-03
K39	9.29371e-03
K40	1.19591e-06
K41	7.05098e-04
Ca40	2.81286e+00
Ca42	1.97112e-02
Ca43	4.21087e-03
Ca44	6.65754e-02
Ca46	1.33465e-04
Ca48	6.51088e-03
<hr/>	
spmc_Fibulae_distal	
H1	9.53781e+00
H2	2.19226e-03
C12	5.05278e+01
C13	5.92189e-01
N14	1.61368e+00
N15	6.31502e-03
O16	2.97591e+01
O17	1.20477e-02
O18	6.88178e-02
Na23	1.50000e-01
Mg24	3.89750e-02
Mg25	5.14005e-03
Mg26	5.88496e-03
P31	2.36000e+00
S32	1.42073e-01
S33	1.15681e-03
S34	6.75336e-03
S36	1.68255e-05
Cl35	7.47256e-03
Cl37	2.52744e-03
K39	9.29371e-03
K40	1.19591e-06
K41	7.05098e-04
Ca40	4.98775e+00
Ca42	3.49517e-02
Ca43	7.46670e-03
Ca44	1.18051e-01
Ca46	2.36659e-04
Ca48	1.15451e-02
<hr/>	
spmc_Ankles_and_feet	
H1	9.54781e+00

H2	2.19456e-03
C12	5.05871e+01
C13	5.92884e-01
N14	1.61368e+00
N15	6.31502e-03
O16	2.97292e+01
O17	1.20356e-02
O18	6.87487e-02
Na23	1.50000e-01
Mg24	3.89750e-02
Mg25	5.14005e-03
Mg26	5.88496e-03
P31	2.34000e+00
S32	1.42073e-01
S33	1.15681e-03
S34	6.75336e-03
S36	1.68255e-05
Cl35	7.47256e-03
Cl37	2.52744e-03
K39	9.29371e-03
K40	1.19591e-06
K41	7.05098e-04
Ca40	4.95875e+00
Ca42	3.47485e-02
Ca43	7.42329e-03
Ca44	1.17365e-01
Ca46	2.35283e-04
Ca48	1.14779e-02
<hr/>	
spmc_Humera_upper_shaft	
H1	1.11774e+01
H2	2.56913e-03
C12	5.48768e+01
C13	6.43160e-01
N14	1.51407e+00
N15	5.92521e-03
O16	3.12351e+01
O17	1.26453e-02
O18	7.22311e-02
Na23	1.00000e-01
Mg24	3.89750e-02
Mg25	5.14005e-03
Mg26	5.88496e-03

P31	1.20000e-01
S32	1.23130e-01
S33	1.00257e-03
S34	5.85291e-03
S36	1.45821e-05
Cl35	1.49451e-02
Cl37	5.05489e-03
K39	9.29371e-03
K40	1.19591e-06
K41	7.05098e-04
Fe54	1.69367e-03
Fe56	2.75705e-02
Fe57	6.48111e-04
Fe58	8.77633e-05
<hr/>	
spmc_Humera_lower_shaft	
H1	1.14674e+01
H2	2.63577e-03
C12	6.25865e+01
C13	7.33518e-01
N14	7.47076e-01
N15	2.92362e-03
O16	2.40746e+01
O17	9.74639e-03
O18	5.56723e-02
Na23	1.00000e-01
P31	1.00000e-01
S32	9.47153e-02
S33	7.71207e-04
S34	4.50224e-03
S36	1.12170e-05
Cl35	7.47256e-03
Cl37	2.52744e-03
<hr/>	
spmc_Radii_shaft	
H1	1.14674e+01
H2	2.63577e-03
C12	6.26063e+01
C13	7.33749e-01
N14	7.47076e-01
N15	2.92362e-03
O16	2.40546e+01
O17	9.73831e-03
O18	5.56262e-02

Na23	1.00000e-01
P31	1.00000e-01
S32	9.47153e-02
S33	7.71207e-04
S34	4.50224e-03
S36	1.12170e-05
Cl35	7.47256e-03
Cl37	2.52744e-03
<hr/>	
spmc_Ulnae_shaft	
H1	1.14774e+01
H2	2.63807e-03
C12	6.26458e+01
C13	7.34213e-01
N14	7.47076e-01
N15	2.92362e-03
O16	2.40147e+01
O17	9.72217e-03
O18	5.55340e-02
Na23	1.00000e-01
P31	1.00000e-01
S32	9.47153e-02
S33	7.71207e-04
S34	4.50224e-03
S36	1.12170e-05
Cl35	7.47256e-03
Cl37	2.52744e-03
<hr/>	
spmc_Femora_upper_shaft	
H1	1.11674e+01
H2	2.56683e-03
C12	5.47879e+01
C13	6.42117e-01
N14	1.51407e+00
N15	5.92521e-03
O16	3.13249e+01
O17	1.26816e-02
O18	7.24386e-02
Na23	1.00000e-01
Mg24	3.89750e-02
Mg25	5.14005e-03
Mg26	5.88496e-03
P31	1.20000e-01
S32	1.23130e-01

S33	1.00257e-03
S34	5.85291e-03
S36	1.45821e-05
Cl35	1.49451e-02
Cl37	5.05489e-03
K39	9.29371e-03
K40	1.19591e-06
K41	7.05098e-04
Fe54	1.69367e-03
Fe56	2.75705e-02
Fe57	6.48111e-04
Fe58	8.77633e-05
<hr/>	
spmc_Femora_lower_shaft	
H1	1.14674e+01
H2	2.63577e-03
C12	6.25469e+01
C13	7.33054e-01
N14	7.47076e-01
N15	2.92362e-03
O16	2.41045e+01
O17	9.75850e-03
O18	5.57415e-02
Na23	1.00000e-01
P31	1.00000e-01
S32	9.47153e-02
S33	7.71207e-04
S34	4.50224e-03
S36	1.12170e-05
Cl35	7.47256e-03
Cl37	2.52744e-03
<hr/>	
spmc_Tibiae_shaft	
H1	1.14674e+01
H2	2.63577e-03
C12	6.25469e+01
C13	7.33054e-01
N14	7.47076e-01
N15	2.92362e-03
O16	2.41145e+01
O17	9.76254e-03
O18	5.57646e-02
Na23	1.00000e-01
P31	1.00000e-01

S32	9.47153e-02
S33	7.71207e-04
S34	4.50224e-03
S36	1.12170e-05
Cl35	7.47256e-03
Cl37	2.52744e-03
<hr/>	
spmc_Fibulae_shaft	
<hr/>	
H1	1.14674e+01
H2	2.63577e-03
C12	6.25766e+01
C13	7.33402e-01
N14	7.47076e-01
N15	2.92362e-03
O16	2.40846e+01
O17	9.75043e-03
O18	5.56954e-02
Na23	1.00000e-01
P31	1.00000e-01
S32	9.47153e-02
S33	7.71207e-04
S34	4.50224e-03
S36	1.12170e-05
Cl35	7.47256e-03
Cl37	2.52744e-03
<hr/>	
Aluminum	
<hr/>	
Al27	1.00000e+02
<hr/>	
Regolith	
<hr/>	
O16	3.61119e-01
O17	1.46196e-04
O18	8.35085e-04
Na23	3.25900e-02
Mg24	6.39190e-02
Mg25	8.42968e-03
Mg26	9.65133e-03
Al27	1.08500e-01
Si28	3.77296e-02
Si29	1.98517e-03
Si30	1.35526e-03
P31	6.39100e-03
S32	3.96763e-02
S33	3.23059e-04
S34	1.88599e-03

S36	4.69880e-06
Cl35	7.81629e-03
Cl37	2.64371e-03
K39	8.07065e-03
K40	1.03852e-06
K41	6.12307e-04
Ca40	1.01205e-01
Ca42	7.09195e-04
Ca43	1.51505e-04
Ca44	2.39534e-03
Ca46	4.80198e-06
Ca48	2.34257e-04
Ti46	1.98636e-03
Ti47	1.83028e-03
Ti48	1.85203e-02
Ti49	1.38747e-03
Ti50	1.35554e-03
Cr50	1.07514e-03
Cr52	2.15610e-02
Cr53	2.49192e-03
Cr54	6.31987e-04
Mn55	3.24000e-03
Fe54	1.83594e-03
Fe56	2.98864e-02
Fe57	7.02552e-04
Fe58	9.51354e-05
Ni58	4.21733e-02
Ni60	1.68045e-02
Ni61	7.42676e-04
Ni62	2.40680e-03
Ni64	6.32647e-04
Zn64	2.31363e-02
Zn66	1.34556e-02
Zn67	1.99012e-03
Zn68	9.22402e-03
Zn70	3.13949e-04
Br79	2.09472e-03
Br81	2.08928e-03
<hr/>	
Atmos1	
H1	2.35800e-07
H2	9.55700e-10
C12	2.57878e-01

C13	3.02234e-03
N14	2.69446e-02
N15	1.05445e-04
O16	6.94114e-01
O17	2.81006e-04
O18	1.60513e-03
Ne20	2.24456e-08
Ne21	7.03344e-11
Ne22	2.52410e-09
Ar36	4.81479e-05
Ar38	9.58184e-06
Ar40	1.59723e-02
Kr78	9.91951e-12
Kr80	6.55123e-11
Kr82	3.40535e-10
Kr83	3.41930e-10
Kr84	1.71478e-09
Kr86	5.32324e-10
Xe124	7.20008e-13
Xe126	6.83973e-13
Xe128	1.49132e-11
Xe129	2.07726e-10
Xe130	3.22798e-11
Xe131	1.69654e-10
Xe132	2.16650e-10
Xe134	8.52959e-11
Xe136	7.34772e-11
